symmetry

Article

# Solving Conformal Mapping Issues in Tunnel Engineering

**Wenbo Chen [1], Dingli Zhang [1,*], Qian Fang [1], Xuanhao Chen [1] and Lin Yu [2]**

[1] Key Laboratory for Urban Underground Engineering of the Education Ministry, Beijing Jiaotong University, Beijing 100044, China; 19115010@bjtu.edu.cn (W.C.); qfang@bjtu.edu.cn (Q.F.); 19115011@bjtu.edu.cn (X.C.)
[2] Beijing Mass Transit Railway Operation Corp., Ltd., Beijing 100044, China; 16115284@bjtu.edu.cn
* Correspondence: dlzhang@bjtu.edu.cn

**Abstract:** The calculation of conformal mapping for irregular domains is a crucial step in deriving analytical and semi-analytical solutions for irregularly shaped tunnels in rock masses using complex theory. The optimization methods, iteration methods, and the extended Melentiev's method have been developed and adopted to calculate the conformal mapping function in tunnel engineering. According to the strict definition and theorems of conformal mapping, it is proven that these three methods only map boundaries and do not guarantee the mapping's conformal properties due to inherent limitations. Notably, there are other challenges in applying conformal mapping to tunnel engineering. To tackle these issues, a practical procedure is proposed for the conformal mapping of common tunnels in rock masses. The procedure is based on the extended SC transformation formulas and corresponding numerical methods. The discretization codes for polygonal, multi-arc, smooth curve, and mixed boundaries are programmed and embedded into the procedure, catering to both simply and multiply connected domains. Six cases of conformal mapping for typical tunnel cross sections, including rectangular tunnels, multi-arc tunnels, horseshoe-shaped tunnels, and symmetric and asymmetric multiple tunnels at depth, are performed and illustrated. Furthermore, this article also illustrates the use of the conformal mapping method for shallow tunnels, which aligns with the symmetry principle of conformal mapping. Finally, the discussion highlights the use of an explicit power function as an approximation method for symmetric tunnels, outlining its key points.

**Keywords:** conformal mapping; tunnel engineering; complex analysis; Schwarz–Christoffel mapping; existence and uniqueness theorem; boundary correspondence theorem



**Citation:** Chen, W.; Zhang, D.; Fang, Q.; Chen, X.; Yu, L. Solving Conformal Mapping Issues in Tunnel Engineering. *Symmetry* **2024**, *16*, 86. https://doi.org/10.3390/sym16010086

Academic Editors: Chong Wang, Yao Bai and Renliang Shan

Received: 30 November 2023
Revised: 4 January 2024
Accepted: 8 January 2024
Published: 10 January 2024



## 1. Introduction

The complex variable approach establishes a connection between harmonic boundary-value problems and the theory of Cauchy contour integrals, serving as an effective and powerful tool for solving plane elastic problems [1,2]. It is used to analyze the mechanical behavior of circular tunnels excavated in rock masses [3,4]. Conformal mapping is used to expand the applicability of this method to a wider range of tunnels with complex shapes. This is achieved by transforming the harmonic boundary-value problem in the general domain into an equivalent boundary-value problem in the circular domain. The latter can be easily solved using the integral method, power series method, or other methods [5].

Kantorovich and Krylov [6] translated the Russian Melentiev's (Мелентьев) method [7], a graphical technique for conformal mapping, into English and further developed the method. Setiawan and Zimmerman [8,9] utilized Melentiev's method to perform a mechanical analysis of a cavity with an arbitrary shape and to study the evolution of a wellbore breakout. Chen [3] introduced Melentiev's method in Chinese for the mechanical analysis of tunnels. Zhang et al. [10] presented an extended Мелентьев method to separately map the lining and surrounding rock separately in order to analytically investigate the elastic mechanical behavior of the lined tunnel.

Chen [3] also introduced an iteration method of trigonometric interpolation for conformal mapping. Exadaktylos et al. [11], Huangfu et al. [12], Zhu et al. [13], Zhou et al. [14], Xu et al. [15], He et al. [16], and Bu et al. [17] proposed similar iteration methods for mapping circular boundaries to tunnel boundaries and performed the mechanical analysis for the irregularly shaped tunnels in rock masses. Tan et al. [18,19] used Zhu's method [13] to calculate the stress around openings in rock masses. Tong et al. [20] derived the complex variable solution for a shallow rectangular tunnel using Zhou's method [14]. Lu et al. [21] and Zhang et al. [22] proposed alternative calculation methods for mapping functions that depend solely on the corresponding relationship between a specific number of control points on boundaries, eliminating the need for iteration.

Lu et al. [23–26] proposed a new mapping method based on an optimization algorithm, complex optimization algorithm, and mixed penalty function algorithm. Qi et al. [27] used the firefly optimization algorithm, a global optimization method inspired by the flashing behavior of fireflies in nature, to map arbitrary stope configurations into unit circles. Li and Liu [28] combined the odd–even point interpolation method with the genetic optimization and a sequential quadratic programming algorithm to map the exterior of the arbitrary excavation cross section in the half-plane to the unit annulus.

These optimization algorithms are widely recognized as methods for implementing conformal mapping and are applied to the study of the analytic analysis of tunnels with complex shapes excavated in rock masses. They are used in research on the mechanical properties and behaviors of rock masses with noncircular cavities [29–31], stress analysis for arbitrarily shaped tunnels in orthotropic rock masses [32], analytic solutions for stress and displacement of noncircular lined tunnels [33–36], analytical solutions for circular tunnels subjected to non-hydrostatic stress considering the elastoplastic interface in rock masses [37,38], analytical solutions for noncircular lined tunnels considering the grouting reinforced area and the frost heaving zone [39–41], analytical stress solutions for an infinite plate with two noncircular holes [42], viscoelastic analysis for stresses and displacements of noncircular sequential excavation [43], and analytical solutions for shallow tunnels with arbitrary shapes in semi-infinite ground [43–45]. Many research papers still present the analytical solution of the noncircular tunnel directly displaying the calculation results without specifying the conformal mapping methods they used [46–53].

However, in the above extended Melentiev's method, iteration methods and optimization methods are developed only based on the point-to-point and boundary-to-boundary correspondence relationships between the circular boundaries and the irregular boundaries, which is inconsistent with the conformal mapping theories (e.g., boundary correspondence principle and existence and uniqueness theorem). And there is no research that can rigorously prove or validate the mapping conformality of these methods.

This paper deeply analyzes and examines the mapping principles and procedures of the extended Melentiev's method, iteration methods, and optimization methods in light of the above contradiction. It also elaborates on their theoretical and graphical problems. Based on the definition of conformal mapping and related theorems and lemmas, the inadequacies of these methods are deduced and demonstrated through reductio ad absurdum and logic inference. To address these challenges in tunnel engineering research, this paper examines and surveys the research on conformal mapping in the field of complex analysis and explores a precise conformal mapping theory with significant practical potential. An exact and practical conformal mapping procedure based on the extended Schwarz–Christoffel transformation is proposed for the mechanical analysis of tunnel engineering. This procedure is applicable to both simply connected domains and multiply connected domains with smooth boundaries, polygon boundaries, polycircular arc boundaries, and mixed boundaries. The proposed procedure performs and presents graphical representations of the conformal mappings of several typical tunnel sections, including the typical symmetric tunnel and the asymmetric tunnel. In the end, the accuracy and practicality of the approximate conformal mapping function expressed by the power series is discussed and verified.

## 2. Materials and Methods

To provide a clear and understandable explanation, several fundamental theorems about conformal mapping in complex analysis are presented first. The conformal mapping in this paper refers to the mapping between canonical circular domains, where the boundaries consist of a group of circles and other domains with the same order of connectivity.

### *2.1. Fundamental Theorems for Conformal Mapping*

The mapping function is defined as conformal on domain $D$ if it can preserve the angles between any two curves. The formal geometric definition of conformal mapping is expressed as follows [54]. If there is an angle $\phi$ and a scale $p > 0$, the function $f(z)$ is conformal at $z_0$ if the map $f$ rotates the tangent vector at $z_0$ by $\phi$ and scales it by $p$ or any smooth curve $\gamma(t)$ through $z_0$. If $f(z)$ is defined on a domain $D$ and is conformal at each point in $D$, it is a conformal map on $D$. The fundamental theorems for conformal mapping are presented in the following subsubsections.

#### 2.1.1. Existence and Uniqueness Theorem

1. Theorem for simply connected domains

The mapping function is defined as conformal on domain $D$ if it can preserve the angles between any two curves. The formal geometric definition of conformal mapping is expressed as follows [55]. Supposing there is an angle $\phi$ and a scale $p > 0$, the function $f(z)$ is conformal at $z_0$ if the map $f$ rotates the tangent vector at $z_0$ by $\phi$ and scales it by $p$ or any smooth curve $\gamma(t)$ through $z_0$. If $f(z)$ is defined on a domain $D$ and is conformal at each point in $D$, it is a conformal map on $D$. The fundamental theorems for conformal mapping are presented in the following subsubsections.

The classical existence and uniqueness theorem, the Riemann mapping theorem [54] states that there exists a unique analytical function $\omega = f(z)$ defined on any simply connected non-degenerate domain $D$ that maps $D$ conformally and univalently onto the open unit disk $|\omega| < 1$ when $f(z_0) = 0$ and $f'(z_0) > 0$ where $z_0 \in D$.

Here is another statement of the existence and uniqueness theorem for conformal mapping from a bounded simply connected domain $D$ onto a disk $|\omega| < 1$ [56]. Suppose $D$ is a bounded domain whose boundary is a Jordan curve $\Gamma$; $z_1$, $z_2$, and $z_3$ are three points on $\Gamma$; $\omega_1$, $\omega_2$, and $\omega_3$ are three points on the circle $|\omega| < 1$; and both sets are arranged in the direction of the positive orientation. Then, there exists a unique function $\omega = f(z)$ that satisfies the following conditions:

(i) $\omega = f(z)$ is univalent and analytic in $D$ and maps $D$ onto the disk.
(ii) $\omega = f(z)$ maps $z_1$, $z_2$, and $z_3$ into $\omega_1$, $\omega_2$, and $\omega_3$, respectively.

In Figure 1, the elliptical domain $D$ is conformally mapped into the circular domains $G_1$ and $G_2$ by $\omega = f_1(z)$ and $\omega = f_2(z)$, respectively, while $z_1$, $z_2$, and $z_3$ on the boundary of the ellipse are mapped to $\omega_1$, $\omega_2$, and $\omega_3$ on the circle $|\omega| = 1$ and $\omega_1^*$, $\omega_2^*$, and $\omega_3^*$ on the circle $|\omega| = r$ ($r$ is an arbitrary positive real number). The conformal functions, both $\omega = f_1(z)$ and $\omega^* = f_2(z)$, exist and are unique, respectively. $G_1$ and $G_2$ belong to one circular domain class, which can be mutually mapped by scaling, translation, rotation, and symmetric transformation of the fractional linear function. Therefore, two corollaries can be derived. There are two main properties of conformal mapping: first, there are numerous functions that can conformally map a bounded simply connected domain into a circular disk domain, and second, only one conformal mapping function exists for a certain circular domain.

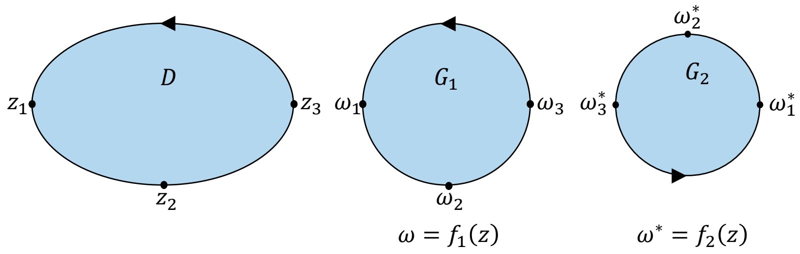


**Figure 1.** Illustration of the existence and uniqueness theorem for a simply connected domain.

2. Theorem for doubly connected domains

According to Wen [54], any doubly connected domain can be conformally mapped onto an annulus $\rho_1 < |\omega| < \rho_2$. The necessary and sufficient condition for the existence of a univalent analytic function that maps the annulus $r_1 < |z| < r_2$ onto the annulus $\rho_1 < |\omega| < \rho_2$ is $\rho_2 r_1 = \rho_1 r_2$.

The conformal mapping between these two annuli is unique if a point $z_0$ on the boundary of the annulus $r_1 < |z| < r_2$ corresponds to a point $\omega_0$ on the boundary of the annulus $\rho_1 < |\omega| < \rho_2$. In Figure 2, $z_0$ is one point on the outer boundary of one doubly connected domain, and $\omega_0$ is one point on the outer boundary of an annulus $r < |\omega| < 1$. There exists a unique conformal function for the doubly connected domain that can map $z_0$ into $\omega_0$.

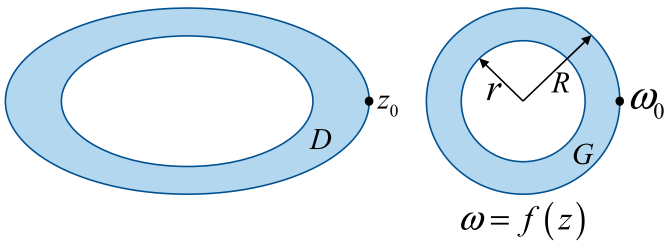


**Figure 2.** Illustration of the existence and uniqueness theorem for a doubly connected domain.

3. Theorem for domains with a higher connectivity

The existence and uniqueness theorem for domains with a higher connectivity is stated as follows [56,57]. Suppose $D$ is an n-connected domain on the z-plane containing infinity. Then, there exists only one univalent meromorphic function $\omega = f(z)$ that can conformally map $D$ onto an n-connected circular domain in the $\omega$-plane. More detailed information is provided by Wen [56], but it is not utilized in this paper.

#### 2.1.2. Boundary Correspondence Principle

The general statement of the boundary correspondence principle in this paper can be summarized as follows [55]. The bounded simply connected domains $D$ and $G$ are enclosed by piecewise smooth, analytic closed curves $\Gamma$ and $L$, respectively. One sufficient condition for the univalence and the conformality of an analytic function, meaning that $\omega = f(z)$ is univalent in $D$ and conformally maps $D$ onto $G$, is that $\omega = f(z)$ is analytic inside $D$ and continuous on $\overline{D} = D \cup \Gamma$ and maps $\Gamma$ bijectively onto $L$.

#### 2.1.3. Functional Properties of the Current Mapping Methods Used in Tunnel Engineering

Conformal mapping functions mapping domains with complex boundaries into circular domains are necessary for obtaining the analytical solution of irregular tunnels. Due to the one-to-one correspondence relation between two domains, the inverse mapping is also conformal. The existence and uniqueness theorem and the boundary correspondence principle are applicable to its inverse mapping.

Numerous explanations and illustrations of mapping methods are found in current tunnel mechanics research [4,13,16,25,27,58]. The functional properties and theoretical defects of these iteration methods and optimization methods are analyzed and inferred in this subsection using conformal mapping from the disk $|\omega| < 1$ onto one ellipse domain.

The conformal mapping function and its inverse function are expressed in finite terms of the Laurent series, as shown in Equations (1) and (2).

$$z = g(\xi) = b_0 + \sum_{k=1}^{l} b_k \xi^k + b_{-k} \xi^{-k}, \tag{1}$$

$$\xi = f(z) = c_0 + \sum_{k=1}^{l} c_k \xi^k + c_{-k} \xi^{-k}, \tag{2}$$

First, set the initial value of the coefficient vector $C_1 = [c_{-k} \cdots c_{-1}\ c_0\ \ c_1 \cdots c_{-k}]$. As shown in Figure 3, Choose $m$ points $\xi_1,\ \xi_2, \cdots \xi_m$ anticlockwise on the boundary of the unit circle $|\xi| < 1$ in the $\xi$-plane. $\xi_1,\ \xi_2, \cdots \xi_m$ are mapped sequentially into $z_1^1,\ z_2^1, \cdots z_m^1$ in the $Z$-plane by the coefficient vector $C_1$. Then, $z_1^1,\ z_2^1, \cdots z_m^1$ and the coefficient vector $C_1$ are updated into $z_1^2,\ z_2^2, \cdots z_m^2$ and $C_2$ through trigonometric interpolation or other ways to decrease the distance between the mapping points and the elliptic boundary. Repeat updating until the distances between $z_1^n,\ z_2^n, \cdots z_m^n$ and the elliptic boundary are small enough after $n$ iterations.

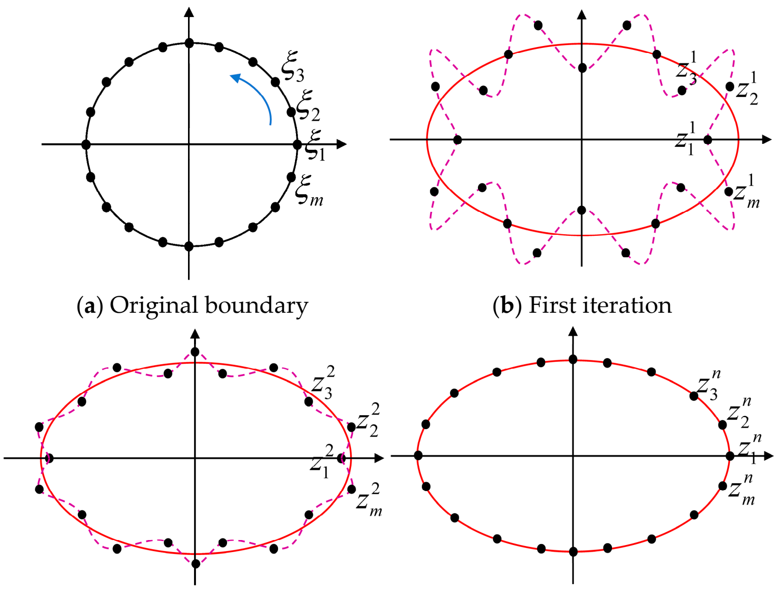

(**a**) Original boundary (**b**) First iteration

(**c**) Second iteration (**d**) n-th iteration

**Figure 3.** Illustration of iteration method for boundary mapping.

From the above illustration, the functional property of these iteration methods can be understood as obtaining a function that maps points on circular boundaries to points on target boundaries without altering their sequences. The objective of the extended Melentiev's method is similar to that of the iteration methods. These optimization methods aim to minimize the distance between mapping points and the target boundary. They use the points' sequence as a constrained condition and then search for an appropriate optimization method. Specifically, the purpose and function of these methods are to realize the mapping between two boundaries.

### *2.2. Inadequacies of Current Mapping Methods in Tunnel Engineering*

This subsection theoretically examines whether the extended Melentiev's method, iteration methods, and optimization methods can realize the conformal mapping between the bounded simply connected domain $D$ with boundary $\Gamma$ and disk domain $G$ with circle boundary $L$. According to the boundary correspondence principle, the mapping function $g(\xi)$ conformally maps $G$ onto $D$ if $g(\xi)$ is analytic inside G and continuous on $\overline{G} = G \cup L$ and maps $L$ bijectively onto $\Gamma$. Thus, we only need to check if the mapping function obtained using these methods can guarantee the bijectivity (one-to-one correspondence) and analyticity.

### 2.2.1. Inadequacies in Satisfying Bijectivity

The mapping function $g(\xi)$ is obtained according to the corresponding relationship between $m$ pairs of points or by minimizing the distance between $m$ pairs of points and the target boundary. Additional points can be used to calculate the mapping function. However, there is no evidence to support the claim that all points on the boundaries can be bijectively mapped onto the target boundary.

The function expressed In Laurent series limit terms may be analytic in simply connected domains, but it does not possess the inherent bijectivity property. For example, the simple power series function $g_1(\xi) = \xi + \xi^2 + \xi^3 + \xi^4$ maps the radial red lines and the blue circular lines in the unit disk $|\xi| \leq 1$ shown in Figure 4a. into the red curves and the blue curves shown in Figure 4b. For $g_2(\xi) = (1+i)\xi + (1-i)\xi^2 + (1+i)\xi^3 + (1-i)\xi^4$, these radial red lines and the blue circular lines are mapped into the red curves and the blue curves in Figure 4c. Obviously, these are not bijective.

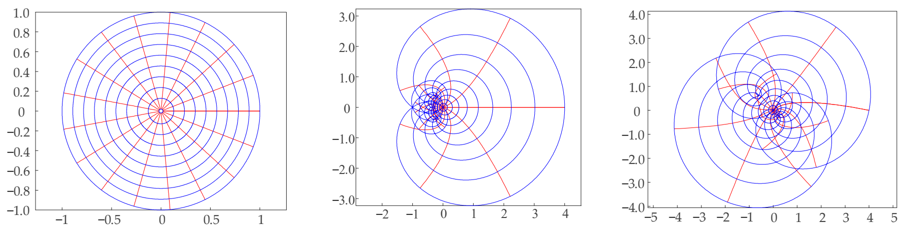

(**a**) Original boundary (**b**) First iteration (**c**) Second iteration

**Figure 4.** Bijectivity test of Laurent series function.

### 2.2.2. Inadequacies in Satisfying Analyticity

Meanwhile, the mapping functions $g(\xi)$ may not be analytical in the mapping domain because there are no restrictive conditions to guarantee analyticity in the calculation process of the iteration and optimization methods. A more rigorous proof is presented as follows.

As shown in Figures 5 and 6, there is one simply connected domain $D_1$ bounded by $\Gamma_1$ and four doubly connected domains $D_2$, $D_3$, $D_4$, and $D_5$ with the same outer boundary $\Gamma_1$ and inner boundaries $\Gamma_2$, $\Gamma_3$, $\Gamma_4$, and $\Gamma_5$. According to the existence and uniqueness theorem for the simply connected domain, one unique conformal mapping function $g_1(\xi)$ maps $D_1$ into the disk $|z| \leq R$. According to the existence and uniqueness theorem for the doubly connected domain, there exist unique functions $g_2(\xi)$, $g_3(\xi)$, $g_4(\xi)$, and $g_5(\xi)$ that can conformally map $D_2$, $D_3$, $D_4$, and $D_5$ into the annulus $r_1 < |z| < R$, $r_2 < |z| < R$, $r_3 < |z| < R$, and $r_4 < |z| < R$, respectively. Definitely, $g_1(\xi)$, $g_2(\xi)$, $g_3(\xi)$, $g_4(\xi)$, and $g_5(\xi)$ can bijectively map the boundary $\Gamma_1$ and $L_1$. It is deduced by reductio ad absurdum that these different functions $g_2(\xi)$, $g_3(\xi)$, $g_4(\xi)$, and $g_5(\xi)$ are not analytic in $D_1$.

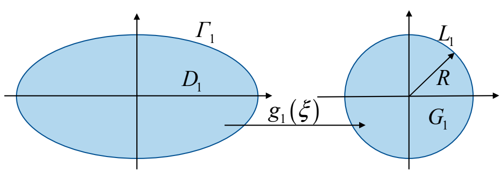


**Figure 5.** Conformal mapping from an elliptic domain into a circular domain.

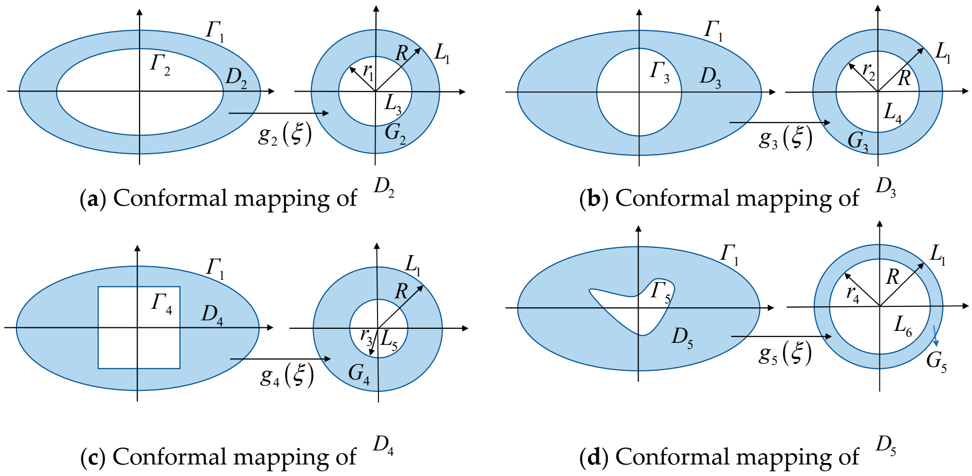


**Figure 6.** Conformal mapping from doubly connected domains into annulus domains.

In summary, there must be numerous functions that can map $\Gamma_1$ and $L_1$ bijectively, injectively, or not. Even if a function is bijective, it might not be a conformal function for the whole domain due to the absence of analyticity. Thus, the function obtained using the iteration and optimization method is just one of many functions, and its conformity for the entire domain is uncertain.

2.2.3. Problems of Applied Range

The classical SC formula was independently discovered by Christoffel in 1867 and Schwarz in 1869. The familiar SC formula is expressed as follows. Suppose $D$ is a bounded domain with a polygonal boundary having vertices $v_1, \cdots, v_n$ and interior angles $\alpha_1\pi, \cdots, \alpha_n\pi$ in counterclockwise order. The formula given in Equation (3) is one conformal mapping function from the unit disk $G$ to $D$.

$$f(z) = A + C\int \prod_{k=1}^{n} \left(1 - \frac{\xi}{z_k}\right)^{\alpha_k - 1} d\xi, \tag{3}$$

where $A$ and $C$ are complex constants, and $v_n = f(z_k)$ for $k = 1, \cdots, n$.

However, a few studies on tunnel mechanics [25,59,60] erroneously apply this SC formula to the conformal mapping of the infinite doubly connected domain (deeply buried tunnels in rock masses) and the finite doubly connected domain (linings or other supporting structures). The correct SC formulas for the conformal mapping of the multiply connected domains are more complex and can be found in the works of Crowdy [61,62] and Delillo et al. [63].

Moreover, some research [33,34,36,40,41,53,64] even uses the same mapping function to map domains that share a single boundary, such as the rock domain, the reinforcement domain, and the lining domain. The root cause of these problems is a common misconception that the mapping is conformal if it can map one domain into a circular domain. For example, the conformal mapping functions of the doubly connected domains in Figure 6 and the infinite domain with one elliptic hole bounded by $\Gamma_1$ are definitely different.

## 3. Rigorous Conformal Mapping Theory in Complex Analysis Field

### *3.1. Evolution of the Conformal Mapping Method and Procedure*

Given the limitations of conformal mapping in tunnel engineering, we look to the advancements in conformal mapping research in the field of complex analysis to find potential solutions. Conformal mapping has been studied for centuries and is carried out using analytical and numerical techniques. The conformal mapping functions between certain domains with simple and regular boundaries can be explicitly expressed, such as the linear function, bilinear function, power function, Joukowski function, exponential and logarithmic functions, and trigonometric functions. Numerous conformal mapping functions are provided by Lavrik and Savenkov [65], Nehari [66], and Ivanov and Trubetskov [57].

When there is no appropriate explicit function for certain complex conformal mappings, numerical calculation is the only option. With the development of computers, fast mapping methods such as Wegmann's method [67,68] have emerged. Although some classical books on numerical conformal mapping [69–73] have been edited and published, the content is relatively abstract and obscure for tunnel engineers. Among the vast amount of literature on conformal mapping, we find a class of methods that is more comprehensible and accessible for tunnel engineering researchers.

Originally, the classical SC formula can only realize the conformal mapping from the unit disk onto a bounded polygonal domain [72]. Then, DeLillo et al. [74] and DeLillo [75] used the reflection principle, while Crowdy [61,62,76,77] used Schottky–Klein prime functions to extend the SC formulas for conformal mappings from circular domains onto unbounded and bounded polygonal domains, respectively. Bauer [78] made some significant contributions to the parameter problem of the SC transformation of conformal mappings from the unit disk onto polygonal domains bounded by circular arcs. Kythe [79] introduced three types of equivalent definitions for SC transformations and discussed several integral equation methods including numerical computation of the Lichtenstein-Gershgorin equation, Theodorsen's integral equation, Symm's integral equation, and Mikhlin's integral equation. The following will present how to implement conformal mapping for tunnel engineering research using the above SC transformation theory.

### *3.2. Construction and Solving of the Boundary Integral Equation*

For the conformal mapping of bounded or unbounded multiply connected domains, the boundary integral equation with the generalized Neumann kernel is constructed firstly based on the parameters of all the boundaries. Then, the integral equation is discretized and solved in the form of linear systems using a common coefficient matrix. The major contents regarding the construction and solving of boundary integral equations for bounded multiply connected domains are presented concisely as follows.

As shown in Figure 7, $G$ is an m-multiply connected domain in a complex plane, and $\alpha$ is a given point in $G$. $G$'s boundary is denoted as $\partial G = \bigcup_{j=1}^{m} \Gamma_j$, where $\Gamma_j$ is the $j$-th closed Jordan curve. Let $J_k$ be the disjoint union $[0, 2\pi]$. The parametrization of the whole boundary $\Gamma$ is defined on $J$ as shown in Equation (4).

$$\eta_k(s) := \begin{cases} \eta_0(s), & s \in J_0 \\ \eta_1(s), & s \in J_1 \\ . & \\ . & \\ \eta_m(s), & s \in J_m \end{cases}, \tag{4}$$

Let $\theta_0, \theta_1, \ldots, \theta_m$ be real constants, and the piecewise constant function $\theta(t)$ is defined as $(\theta_0, \theta_1, \ldots, \theta_m)$, $t \in J_m$. The complex function $A(t)$ and its conjugate $\overline{A(t)}$ are defined on $\Gamma$ as shown in Equations (5) and (6).

$$A(t) = e^{i(\pi/2 - \theta(t))}(\eta(t) - \alpha), \tag{5}$$

$$\overline{A(t)} = \frac{\eta'(t)}{A(t)}, \tag{6}$$

The generalized Neumann kernel formed with $A(t)$ and $\eta$ is defined on $J \times J$ as shown in Equations (7) and (8).

$$N(s,t) := \frac{1}{\pi} \mathrm{Im}\left( \frac{A(s)}{A(t)} \frac{\eta'(t)}{\eta(t) - \eta(s)} \right), \tag{7}$$

$$M(s,t) := \frac{1}{\pi}\mathrm{Re}\left(\frac{A(s)}{A(t)}\frac{\eta'(t)}{\eta(t)-\eta(s)}\right), \tag{8}$$

Let $H$ be the space of all real-valued Hölder continuous functions on the boundary $\Gamma$. The following operators are defined on $H$ as shown in Equations (9)–(11).

$$N\mu(s) := \int_J N(s,t)\mu(t)\mathrm{d}t, \quad s \in J, \tag{9}$$

$$M\mu(s) := \int_J M(s,t)\mu(t)\mathrm{d}t, \quad s \in J, \tag{10}$$

$$J\mu(s) := \int_J \delta(s,t)\mu(t)\mathrm{d}t, \quad s \in J, \tag{11}$$

More detailed properties of the generalized Neumann kernel function and integral operator can be found in refs. [80–83]. The boundary integral equation for the boundary of the multiply connected finite domain is expressed as shown in Equation (12) with the generalized Neumann kernel functions $M$ and $N$.

$$(I-N)\mu = -M\gamma, \tag{12}$$

Since $\int_J N(s,t)\mathrm{d}t = -1$ and $\int_J M(s,t)\mathrm{d}t = 0$, Equation (12) can be written as Equation (13):

$$2\mu(s) - \int_J N(s,t)[\mu(t)-\mu(s)]\mathrm{d}t = -\phi(s), \tag{13}$$

where $\phi(s) = \int_J M(s,t)[\gamma(t)-\gamma(s)]\mathrm{d}t$.

Let vector $t = (t_1, t_2, \ldots, t_{(m+1)n})^{\mathrm{T}}$ and the integral equation Equation (13) be discretized as Equation (14).

$$2\mu(t_i) - \frac{2\pi}{n}\sum_{j=1}^{(m+1)n} N(t_i,t_j)[\mu(t_j)-\mu(t_i)] = -\phi(t_i), \tag{14}$$

where $i = 1, 2, \ldots, (m+1)n$.

Set $x = \mu(t)$ and $y = \phi(t)$. Let $B$ be the $(m+1)n \times (m+1)n$ matrix with the following elements:

$$(\mathrm{B})_{ij} = \begin{cases} 0 & if\ i = j \\ \frac{2\pi}{\mathrm{n}}N(t_i,t_j) & if\ i \neq j \end{cases}, \tag{15}$$

where $i, j = 1, 2, \ldots, (m+1)n$.

The boundary integral equation is transformed by the following $(m+1)n \times (m+1)n$ linear system.

$$(2\mathrm{I} + diag(\mathrm{B}) - \mathrm{B})x = -y, \tag{16}$$

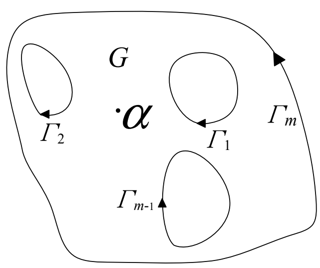


**Figure 7.** Bounded multiply connected domain.

### 3.3. Discretization of Piecewise Smooth Boundary

In tunnel engineering research, the boundaries of common tunnels in rock, such as rectangular tunnels and horseshoe-shaped tunnels, are piecewise smooth with vertices.

Therefore, this paper focuses on the conformal mapping of domains with piecewise smooth boundaries. The following describes the processing method for the boundary at the vertex.

There are $p_j$ vertices $\eta_j\left(c_{j,k}\right)$ on boundary $\Gamma_j$. Then, suppose that $\gamma(t)$ is smooth in each interval $J_j$ except at $p_j \geq 1$ points:

$$c_{j,k} = (k-1)\frac{2\pi}{p_j} \in J_j, \tag{17}$$

where $k = 1, 2, \ldots, p_j, \ \ j = 0, 1, \ldots, m.$

The bijective, strictly monotonically increasing and infinitely differentiable function $\omega(t)$ is defined as shown in Equation (18):

$$\omega(t) = 2\pi\frac{[v(t)]^{p^*}}{[v(t)]^{p^*} + [v(2\pi - t)]^{p^*}}, \tag{18}$$

where $v(t) = (1/p^* - 1/2)(1 - t/\pi)^3 + (t/\pi - 1)/p^* + 1/2\,,\ t \in [0, 2\pi]$, take the grading parameter $p^*$ equal to 3 in this paper.

Set the function $\delta_j(t) = \omega\left(p_j\left(t - c_{j,k}\right)\right)/p_j + c_{j,k},\ t \in [c_{j,k}, c_{j,k+1}]$, and $\delta_j$ satisfies the following:

$$\begin{array}{ll} \delta_j'\left(c_{j,k}\right) = 0, & k = 1, 2, \ldots, p_j, \\ \delta_j'\left(c_{j,k}\right) \neq 0, & t \in J_j - \left\{c_{j,1}, c_{j,2}, \ldots, c_{j,p_j}\right\} \end{array}, \tag{19}$$

Substituting $t = \delta(\tau)$ into the integral $\int_J \gamma(t)\mathrm{d}t$ and set $\hat{\gamma}(\tau) = \gamma(\delta(\tau))\delta'(\tau)$, thus $\hat{\gamma}(0) = \hat{\gamma}(2\pi) = 0$ and $\int_J \gamma(t)\mathrm{d}t = \int_J \gamma(\delta(\tau))\delta'(\tau)\mathrm{d}\tau = \int_J \hat{\gamma}(\tau)\mathrm{d}\tau$. Using the trapezoidal rule, the integral function is transformed into the following:

$$\int_J \gamma(t)\mathrm{d}t \approx \frac{2\pi}{\mathrm{n}}\sum_{k=0}^{m}\sum_{p=1}^{n}\hat{\gamma}\left(s_{k,p}\right) = \frac{2\pi}{\mathrm{n}}\sum_{j=1}^{(m+1)n}\hat{\gamma}\left(t_j\right) = \frac{2\pi}{\mathrm{n}}\sum_{j=1}^{(m+1)n}\hat{\gamma}\left(\delta\left(t_j\right)\right)\delta'\left(t_j\right). \tag{20}$$

## 4. Proposed Conformal Mapping Procedure and Application Cases

Nasser [84–89], Delillo and Kropf [90], Al-Hatemi et al. [88], and Yunus et al. [91] developed the corresponding numerical methods for solving these established integration equations. More numerical methods for conformal mapping are presented by Luo et al. [92], Liesen et al. [93], Gopal and Trefethen [94], and Trefethen [95]. On the basis of SC transformation, Trefethen [96,97] developed one SC transformation procedure Fortran package SCPACK, while Driscoll [72,98–100] created SC Toolbox, a MATLAB package that can compute the conformal mapping from the unit disk onto a given polygonal simply connected domain. Additionally, Nasser [101] developed the MATLAB toolbox PlgCirMap for implementing the conformal mapping from a given polygonal multiply connected domain onto a circular multiply connected domain and its inverse mapping.

Due to the complex shape of the tunnel boundary and the need for explicit conformal mapping in analytical calculations of tunnels in rock masses, the above procedures cannot be directly applied. A mechanical analysis of tunnels in rock masses based on complex function theory requires obtaining the conformal mapping functions for the following three main categories of conformal mapping and their inverse mappings: (i) from the concentric circle domain to the doubly connected polygonal domain, polycircular arc domain, and other domains with piecewise smooth boundaries; (ii) from the infinite circular domain with two or more connectivity numbers to the infinite multiply connected domain with piecewise smooth boundaries; (iii) from the unit disk domain to the bounded simply connected domain with piecewise smooth boundaries.

This section refers to the following materials: the mathematical framework includes function theory, the construction of the SC mapping formulas for bounded and unbounded multiply connected domains, Cauchy transforms, etc. [61,62,74,75,77]; the construction and solving of the integral equation employ the generalized Neumann kernel [84,86–89,102,103] and the discretization of the parametrization of the piecewise smooth boundary with the vertices including the trapezoidal rule and the Nyström method [104–106]; and the procedure framework and the MATLAB functions include CIRMAPB, CIRMAPU, EVALU, EVALUD, etc. [84,85,87,101]. We propose a new procedure, the flow diagram of which is shown in Figure 8, involving a series of integration, extension, and upgrading steps.

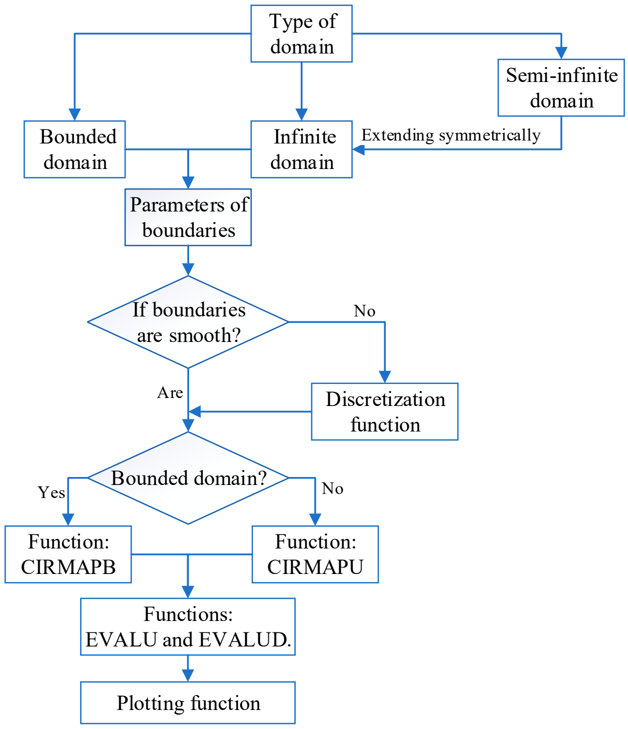


**Figure 8.** Flow diagram of the conformal mapping procedure.

This procedure can handle the process of conformal mapping for three typical types of tunnels. If the rock domain is semi-infinite, it should first be extended into the infinite domain according to the symmetry principle of conformal mapping [57]. For domains with smooth boundaries, the conformal mapping functions EVALU and the inverse mapping functions EVALUD can be obtained using the CIRMAPB function for bounded domains and the CIRMAPU function for unbounded domains. If any boundary of the domain is piecewise smooth, the boundary with vertices should be discretized using the discretization function. As an innovation of this article, we provide three discretization functions to handle polygon boundaries, polycircular arc boundaries, and mixed boundaries, respectively, based on the theory provided in Section 3.3. This approach has a broader range of applications compared to previous procedures. In the plotting module, images of canonical circular domains and original domains with rectangular orthogonal curves or polar orthogonal curves are plotted first. Then, images conformally mapped from these curves are plotted. More details can be found in Supplementary Materials, which provide Main procedure codes of conformal mapping for the lining domain in Case 4.

In order to demonstrate the usefulness and practicality of the procedure in tunnel engineering, six typical domains of deeply buried tunnels are mapped using conformal mapping, and the mapping of a shallow tunnel is also conducted. The following seven cases are illustrated. The blue curves and red curves before mapping are orthogonal. Firstly, this mapping should maintain the shape and size of the original domain and the circularity of the circular domain. The conformal mapping can be tested based on two other criteria which satisfy the angle preservation property and bijectivity. The first criterion satisfying conformality is that the blue curves and red curves after mapping are also orthogonal. The second criterion satisfying bijectivity is that any two different points will not overlap after mapping. It is obvious that the proposed procedure works well based on the mapping figures shown in Case 1–Case 7.

Case 1: rectangular tunnel

The first type consists of an infinite rock domain with a rectangular hole and a lining domain with a rectangular ring shape. The physical dimensions are indicated in Figure 9. Figures 10 and 11 depict the conformal mapping and its inverse conformal mapping, respectively, illustrating the curves in the rock domain before mapping and after mapping. Figures 12 and 13 depict the conformal mapping and its inverse conformal mapping, respectively, illustrating the curves in the lining domain before mapping and after mapping. The curves depicted in this paper are represented by closely spaced dots.

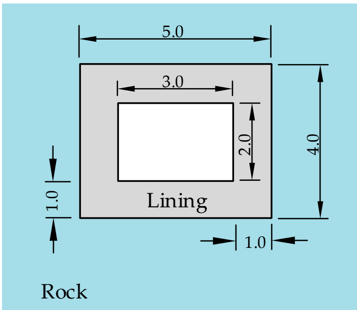


**Figure 9.** Tunnel sectional drawing of Case 1.

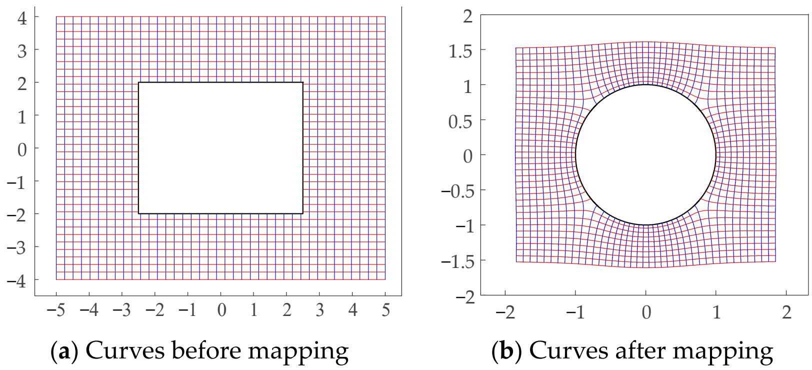


**Figure 10.** Conformal mapping of the rock domain in Case 1.

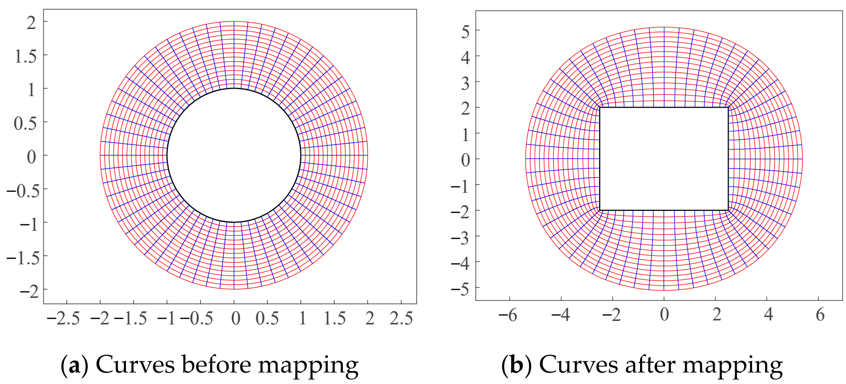


**Figure 11.** Inverse conformal mapping of the rock domain in Case 1.

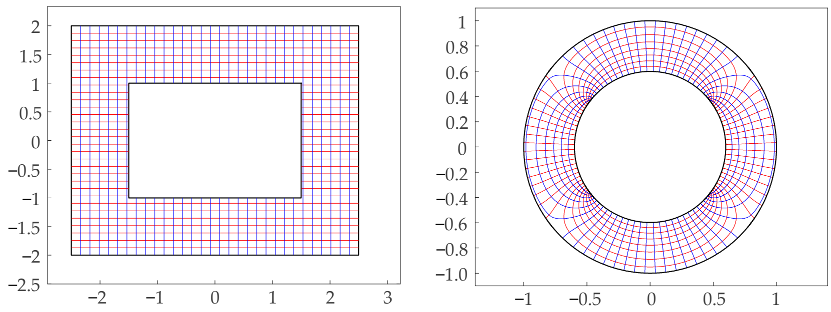

(**a**) Curves before mapping (**b**) Curves after mapping

**Figure 12.** Conformal mapping of the lining domain in Case 1.

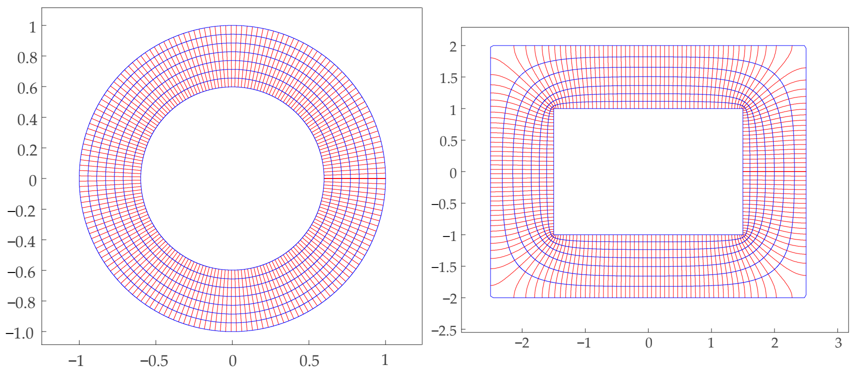

(**a**) Curves before mapping (**b**) Curves after mapping

**Figure 13.** Inverse conformal mapping of the lining domain in Case 1.

Case 2: rectangular tunnels with reinforcement

The arch crown of rock masses in Case 1 is reinforced as for the second type, with a fan-shaped reinforced area and polygonal lining. The physical dimensions of Case 2 are indicated in Figure 14. Figures 15 and 16 depict the curves mapped conformally and inversely in an infinite rock domain with mixed boundaries of arcs and lines. Figures 17 and 18 depict the curves mapped conformally and inversely in a finite reinforcement domain with mixed boundaries. Figures 19 and 20 depict the curves mapped conformally and inversely in a finite lining domain.

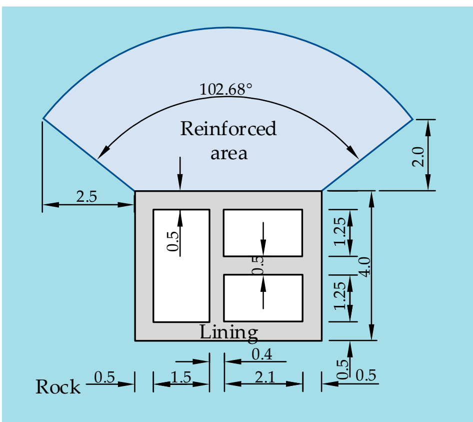


**Figure 14.** Tunnel sectional drawing of Case 2.

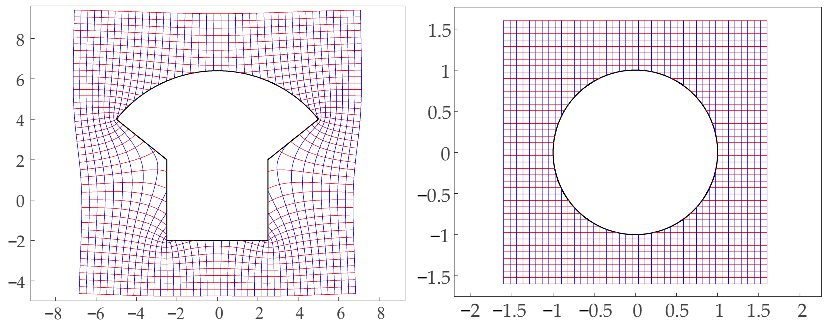


(**a**) Curves before mapping (**b**) Curves after mapping

**Figure 15.** Conformal mapping of the rock domain in Case 2.

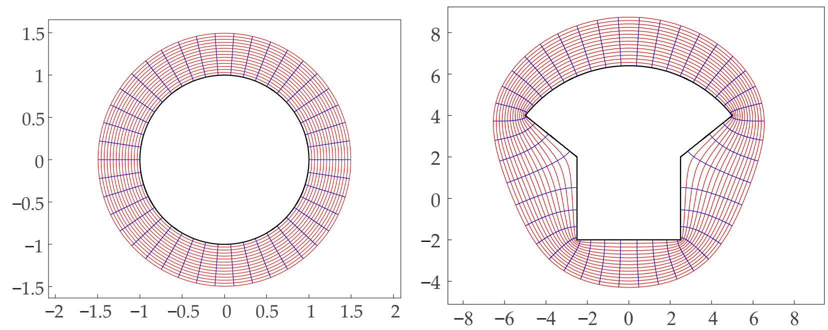


(**a**) Curves before mapping (**b**) Curves after mapping

**Figure 16.** Inverse conformal mapping of the rock domain in Case 2.

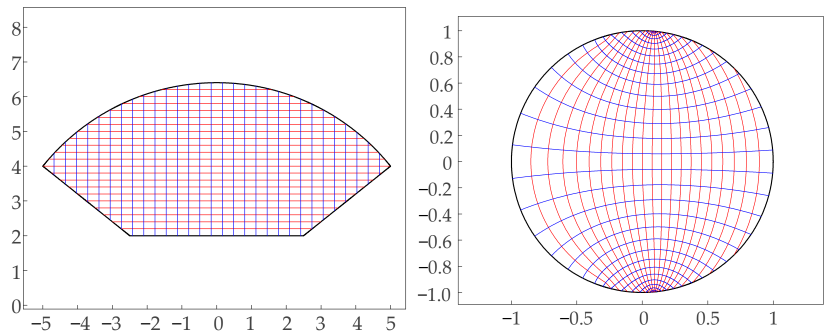


(**a**) Curves before mapping (**b**) Curves after mapping

**Figure 17.** Conformal mapping of the reinforcement domain in Case 2.

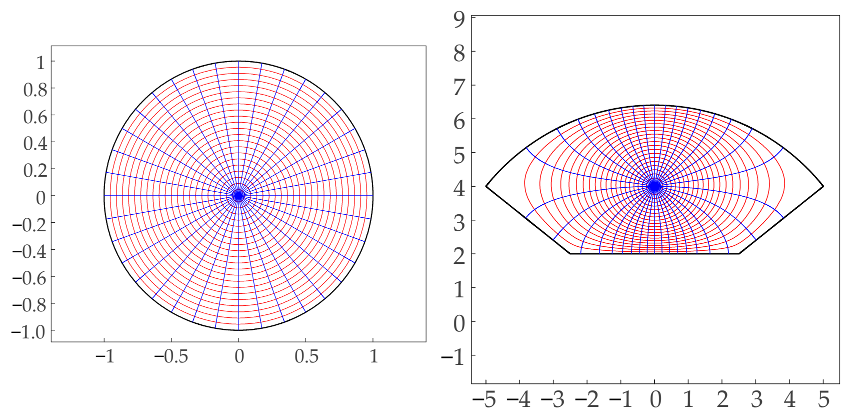


(**a**) Curves before mapping (**b**) Curves after mapping

**Figure 18.** Inverse conformal mapping of the reinforcement domain in Case 2.

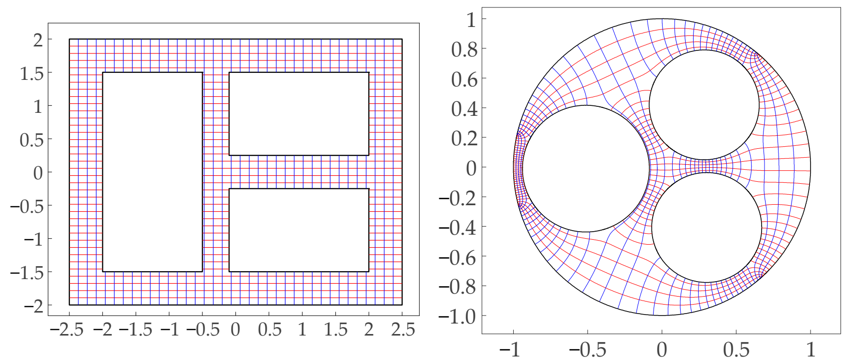


(**a**) Curves before mapping (**b**) Curves after mapping

**Figure 19.** Conformal mapping of the lining domain in Case 2.

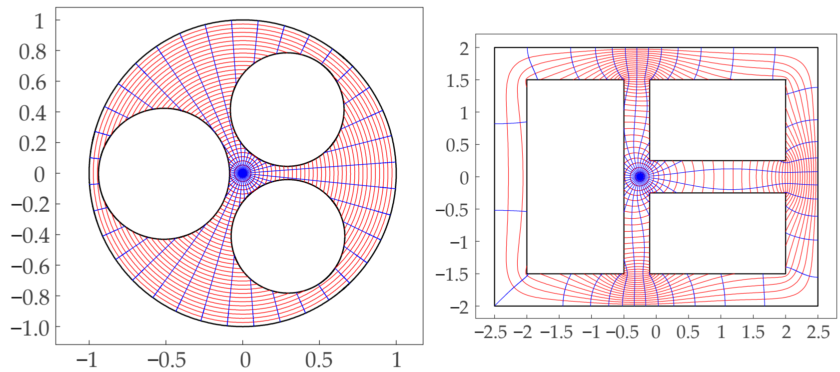


(**a**) Curves before mapping (**b**) Curves after mapping

**Figure 20.** Inverse conformal mapping of the lining domain in Case 2.

Case 3: multiarc tunnel

The third case is one typical railway tunnel. The physical dimensions of this multiarc tunnel cross section are indicated in Figure 21. Figures 22–24 depict the conformal mapping and inverse conformal mapping of finite and infinite doubly connected domains with polycircular arc boundaries. The curves mapped conformally and inversely are the same because of the geometrical similarity of the curves in the lining domain.

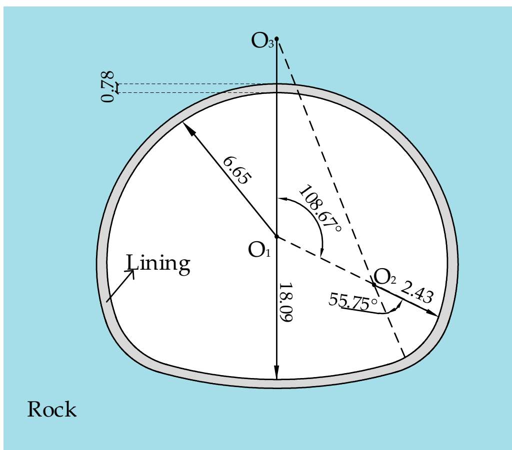


**Figure 21.** Tunnel sectional drawing of Case 3.

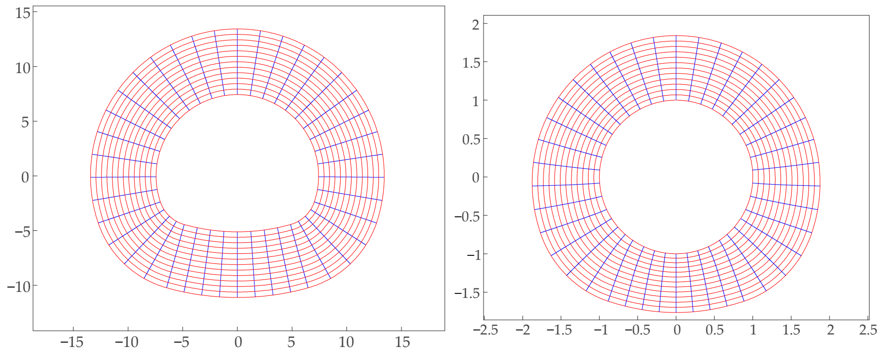


(**a**) Curves before mapping (**b**) Curves after mapping

**Figure 22.** Conformal mapping of the rock domain in Case 3.

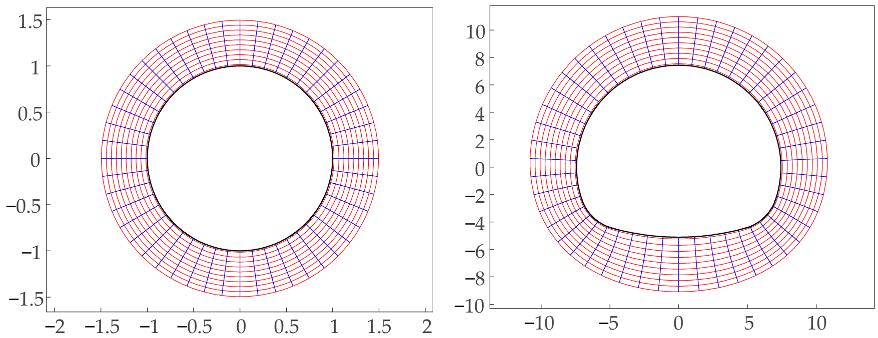


(**a**) Curves before mapping (**b**) Curves after mapping

**Figure 23.** Inverse conformal mapping of the rock domain in Case 3.

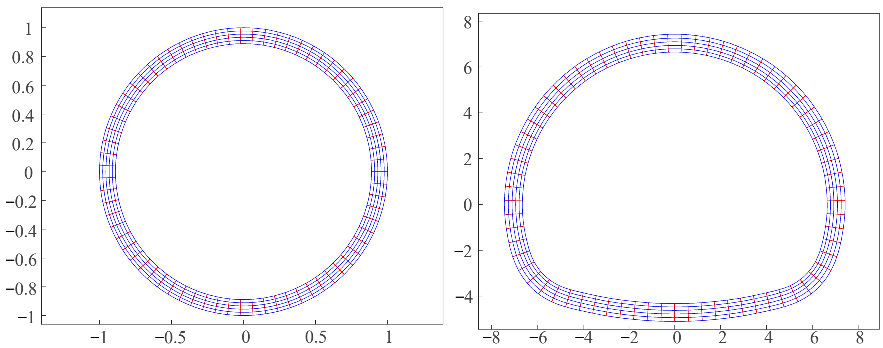


(**a**) Curves before mapping (**b**) Curves after mapping

**Figure 24.** Conformal mapping and inverse mapping of the lining domain in Case 3.

Case 4: horseshoe-shaped tunnel

The fourth case is a typical horseshoe-shaped tunnel. The physical dimensions of this tunnel cross section are indicated in Figure 25. Figures 26 and 27 depict the conformal mapping and inverse conformal mapping of the infinite rock domain with mixed boundaries of arcs and lines. Figures 28 and 29 depict the conformal mapping and inverse conformal mapping of the finite lining domain with mixed boundaries of arcs and lines.

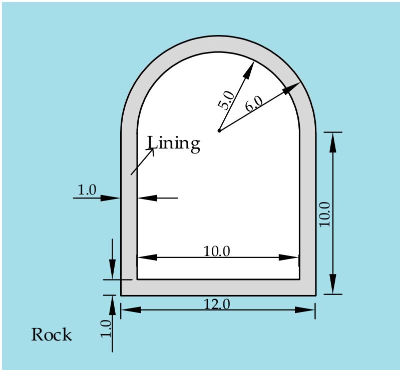


**Figure 25.** Tunnel sectional drawing of Case 4.

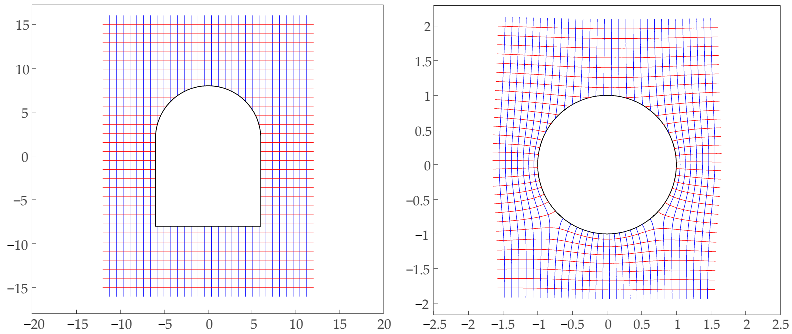

(**a**) Curves before mapping (**b**) Curves after mapping

**Figure 26.** Conformal mapping of the rock domain in Case 4.

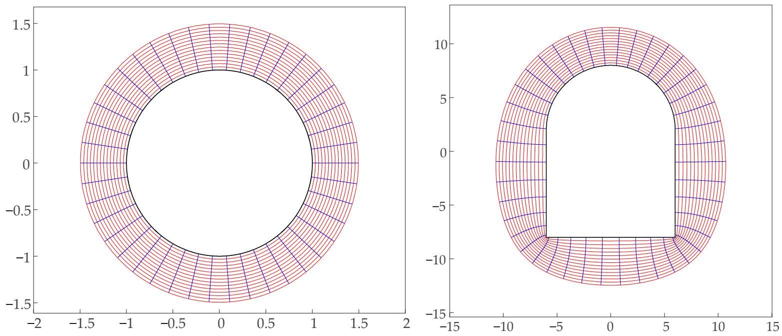

(**a**) Curves before mapping (**b**) Curves after mapping

**Figure 27.** Inverse conformal mapping of the rock domain in Case 4.

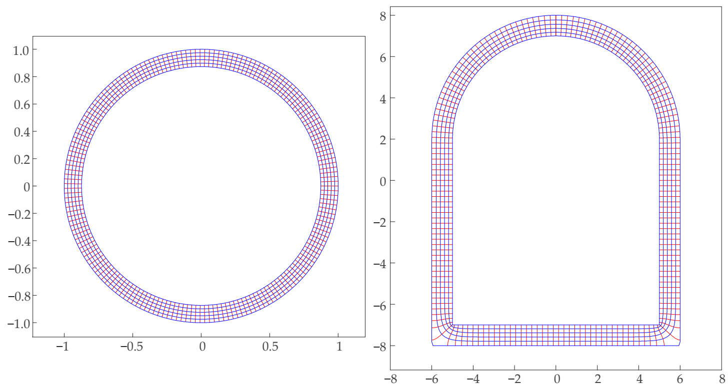

(**a**) Curves before mapping (**b**) Curves after mapping

**Figure 28.** Inverse conformal mapping of the rock domain in Case 4.

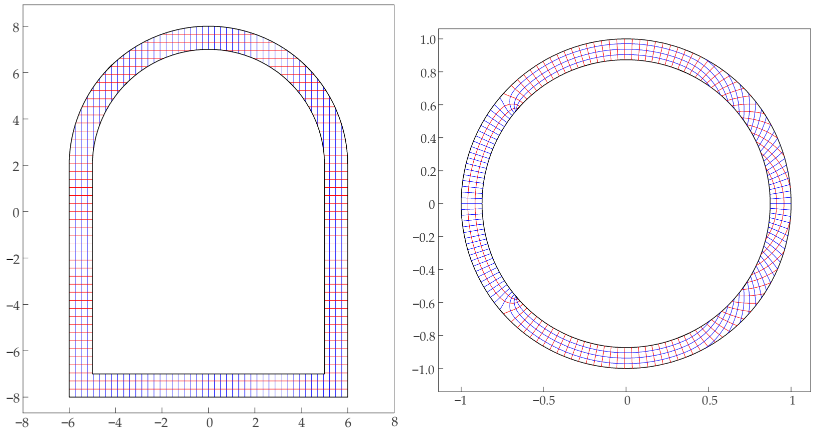


(**a**) Curves before mapping (**b**) Curves after mapping

**Figure 29.** Conformal mapping of the lining domain in Case 4.

Case 5: multiple holes in rock masses

The fifth case is an infinite rock with multiple holes, of which the boundaries are smooth. The functions of the boundaries in Figure 30 can be expressed in the complex plane as follows.

Boundary 1:

$$z_1 = \cos(t) - 0.4i\sin(t),\ t \in [0, 2\pi], \tag{21}$$

Boundary 2:

$$z_2 = 2.5 + \cos(t) + 0.5\cos(2t) - 0.4i\sin(t),\ t \in [0, 2\pi], \tag{22}$$

Boundary 3:

$$z_3 = -1 + 2i + r(t)\cos(t) - ir(t)\sin(t),\ t \in [0, 2\pi], \tag{23a}$$

$$r(t) = 1 + 0.05\cos(t) + 0.1\cos(2t) + 0.075\sin(t) + 0.4\sin(2t),\ t \in [0, 2\pi], \tag{23b}$$

Boundary 4:

$$z_4 = -2i + 0.5\cos(t) - i\sin(t),\ t \in [0, 2\pi], \tag{24}$$

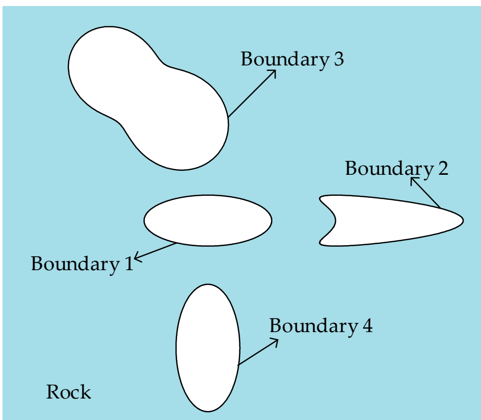


**Figure 30.** Sectional drawing of Case 5.

Given the complexity of the boundaries, only the curves in the rock domain that are mapped inversely conformally are depicted in Figure 31.

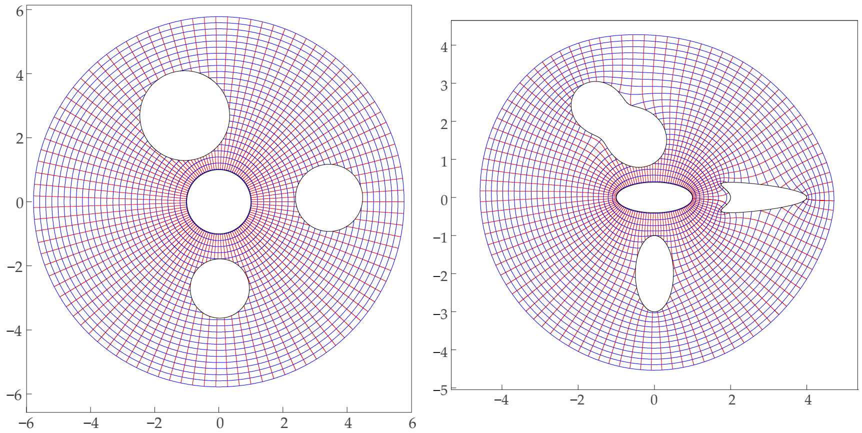

(**a**) Curves before mapping (**b**) Curves after mapping

**Figure 31.** Inverse conformal mapping of the rock domain in Case 5.

Case 6: twin tunnels with a service tunnel

There are two parallel main tunnels and one service tunnel at great depths in Case 6. The physical dimensions of this cross section are indicated in Figure 32. The curves in the infinite rock domain with several mixed boundaries are mapped inversely conformally, as depicted in Figure 33.

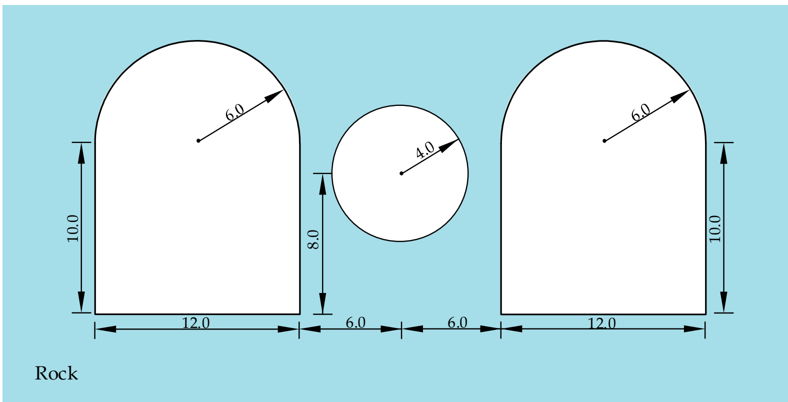


**Figure 32.** Tunnel sectional drawing of Case 6.

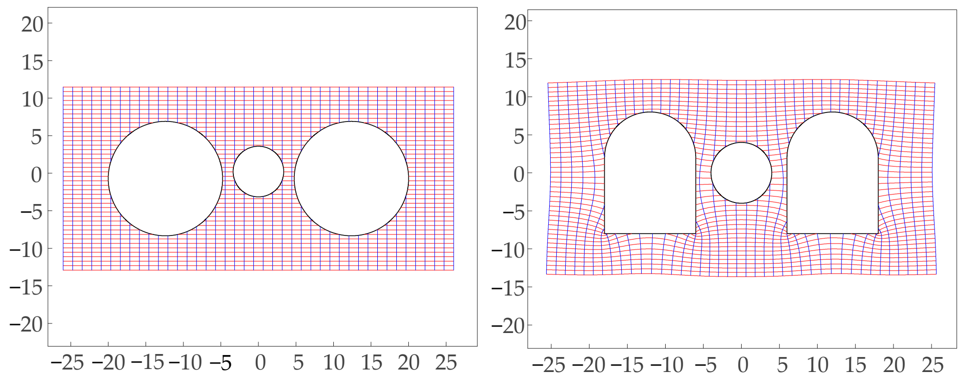

(**a**) Curves before mapping (**b**) Curves after mapping

**Figure 33.** Inverse conformal mapping of the rock domain in Case 6.

Case 7: shallow tunnels

This procedure is also applicable to shallow tunnels. First, the half plane is expanded into one infinite plane symmetrically and then is mapped conformally. Based on the symmetry principle of conformal mapping [57], conformal mapping from the half plane with multiple holes into the half plane with circular holes can be obtained. For conformal mapping from the ring domain onto the half plane with one circular hole, as shown in Figure 34, the appropriate conformal mapping function is expressed as follows [107,108]:

$$z = g(\xi) = -ih\frac{1-\alpha^2}{1+\alpha^2}\frac{1+\xi}{1-\xi}, \tag{25}$$

From the definition of conformal mapping, it is obvious that the composite function of two conformal mapping functions is still a conformal mapping function. Thus, this transformation can satisfy the computing requirements for the mechanical analysis of multiple shallow cavities [109–114].

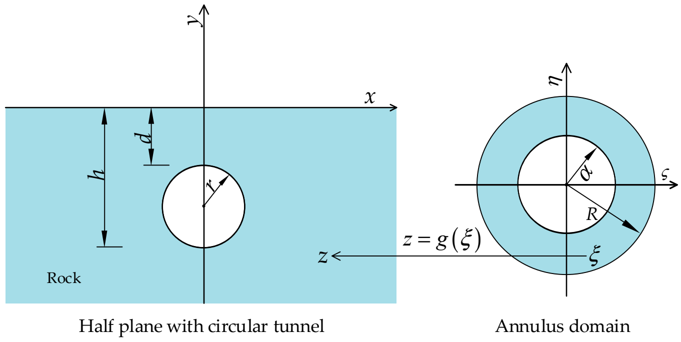


**Figure 34.** Conformal mapping for a shallow circular tunnel.

For example, there is one rectangular tunnel close to the circular tunnel in the half plane, as shown in Figure 35. The half plane is expanded symmetrically by taking the ground level as the axis of symmetry. Then, this infinite plane with four irregular holes is mapped into one with four circular holes, and its inverse mapping is obtained. The curves in the rock domain are depicted in Figures 36 and 37. The axis of symmetry, the curve of the ground level, remains in its middle location during conformal mapping and inverse conformal mapping.

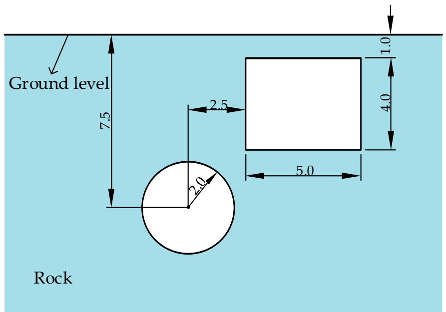


**Figure 35.** Tunnel sectional drawing of Case 7.

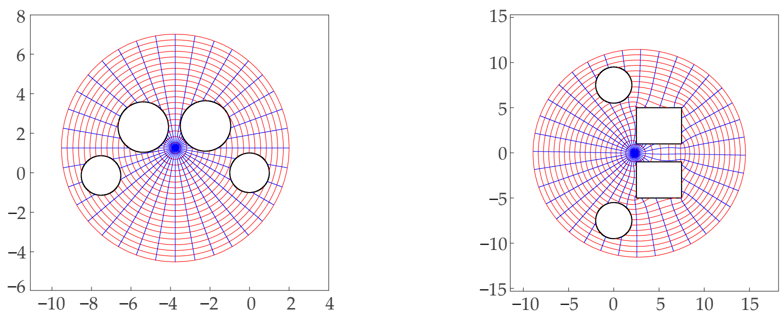


(**a**) Curves before mapping (**b**) Curves after mapping

**Figure 36.** Inverse conformal mapping of the rock domain in Case 7.

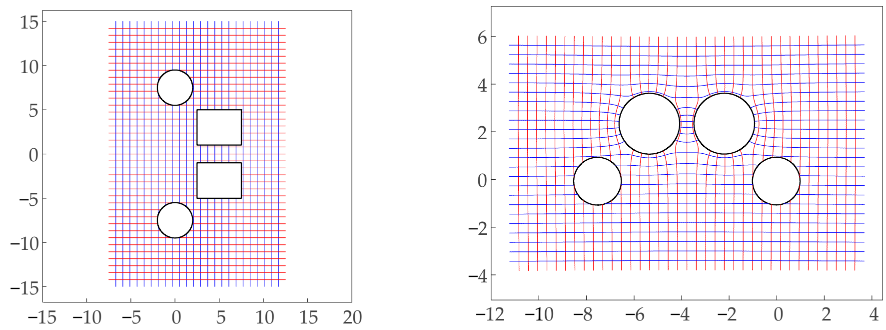

(**a**) Curves before mapping (**b**) Curves after mapping

**Figure 37.** Conformal mapping of the rock domain in Case 7.

## 5. Discussion and Verification of the Application of the Proposed Procedure

The proposed conformal mapping procedure uses a discrete numerical integration method and can conformally map curves in one domain into curves in a circular domain. This can satisfy the demand for calculating the stress functions that only need the points' locations before and after mapping [115]. However, it is still essential to obtain the explicit form of the conformal mapping function for the frequently used integral method and series expansion method [116–120].

Generally, the conformal mapping is approximated by a finite number of items of the power series, as shown in Equation (1). The coefficients of the series function can be calculated according to the corresponding relationship between numerous pairs of points before and after conformal mapping. Obviously, the points not only on the boundary but also in the inner domain should be used to calculate the coefficients with enough accuracy to approximate the conformal mapping of the whole domain. Meanwhile, the approximation quality is greatly affected by the item number of the Laurent series. For the approximation mapping of the rock domain in Case 3, 520 pairs of points on the circular domain and rock domain are selected to calculate the coefficients of the mapping function using the least square method. The approximation conformal mapping function when $l = 20$ is listed as shown in Equation (26), where items for which the module value of the coefficients is less than $10^{-4}$ are omitted. The points mapped using Equation (9) from 13, 600 points on the annulus domain $1 \le |r| \le 2$ in Figure 38a are plotted in Figure 38b.

$$\begin{aligned} z = g(\xi) = {} & 7.0030\xi - 0.7729 - 0.5812\xi^{-1} - 0.3629\xi^{-2} - 0.1747\xi^{-3} - 0.0502\xi^{-4} \\ & +0.0082\xi^{-5} + 0.0208\xi^{-6} + 0.0138\xi^{-7} + 0.0055\xi^{-8} + 0.0020\xi^{-9} + 0.0015\xi^{-10} - 0.0015\xi^{-12} \\ & -0.0031\xi^{-13} - 0.0029\xi^{-14} - 0.0010\xi^{-15} + 0.0016\xi^{-17} + 0.0012i\xi^{-18} \end{aligned}, \quad (26)$$

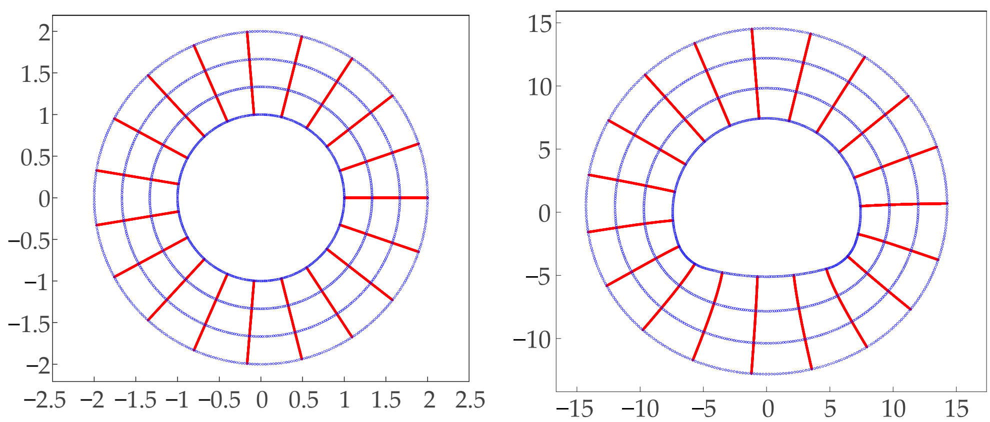

(**a**) points before mapping (**b**) points after mapping

**Figure 38.** Illustration of approximate conformal mapping of the rock domain in Case 3.

The distance between the points mapped using the procedure and the series function separately is used to evaluate the approximation error. In Figure 39, the mean ($M_1$) and the variation coefficient ($COV_1$) of the distances between 13, 600 pairs of points are plotted. The approximation error significantly reduces with the increase in the item number. When the item number of the series function is up to 40, the magnitude orders of $M_1$ and $COV_1$ are $10^{-4}$ and $10^{-8}$, respectively, which are small and accurate enough for the approximation.

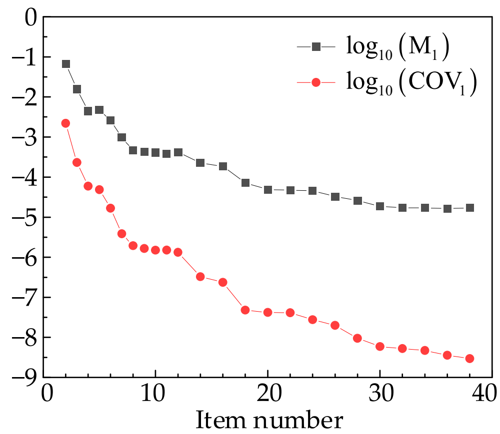


**Figure 39.** Approximation error for approximate conformal mapping of the rock domain in Case 3.

Some researchers think that only a few items of the series function can approximate the conformal mapping well [25,35,117]. For the horseshoe-shaped tunnel section in Case 4, Lu et al. [33,34] proposed the mapping function given in Equation (27) to map the lining domain and the rock domain.

$$z = g(\xi) = 7.54561\big(\xi - 0.07499 + 0.12076\xi^{-1} + 0.04536\xi^{-2} - 0.06513\xi^{-3} + 0.02083\xi^{-4} + 0.00118\xi^{-5} - 0.00285\xi^{-6} - 0.00096\xi^{-7} - 0.00221\xi^{-8}\big), \quad (27)$$

Likewise, we use the Laurent series to approximate the conformal mapping of the rock domain in Case 4 performed using the procedure. A total of 520 pairs of points on the circular domain and the rock domain are selected to calculate the coefficients of the mapping function using the least square method. The approximate conformal mapping function when $l = 20$ is listed as shown in Equation (28).

$$\begin{aligned} z = g(\xi) = {} & 7.7437\xi + 0.7590 + 0.9653\xi^{-1} - 0.5406\xi^{-2} - 0.7765\xi^{-3} - 0.3026\xi^{-4} \\ & + 0.0225\xi^{-5} + 0.0582\xi^{-6} + 0.0458\xi^{-7} + 0.0498\xi^{-8} + 0.0190\xi^{-9} - 0.0179\xi^{-10} \\ & - 0.0211\xi^{-11} - 0.0121\xi^{-12} - 0.0080\xi^{-13} + 0.0010\xi^{-14} + 0.0104\xi^{-15} + 0.0089\xi^{-16} \\ & + 0.0027\xi^{-17} - 0.0003\xi^{-18} - 0.0032\xi^{-19} \end{aligned} \quad (28)$$

Figure 40b,c show 8000 points mapped using approximate conformal mapping functions with $l$ = 8 and $l$ = 20 from 13, 600 points on the annulus domain $1 \le |r| \le 2$ in Figure 40a. Figure 40d shows the points mapped using Lu's function in Equation (10). The accuracy of the approximate conformal mapping based on the proposed procedure is intuitively higher than the previous method.

In Figure 41, the approximation error from 8000 pairs of points drops dramatically with the increment of the item number. When the item number of the series function is up to 40, the magnitude orders of $M_2$ and $COV_2$ are $10^{-3}$ and $10^{-6}$, respectively, which also are small and accurate enough for the approximation. The approximate error can be further decreased by selecting more pairs of points to calculate the coefficients.

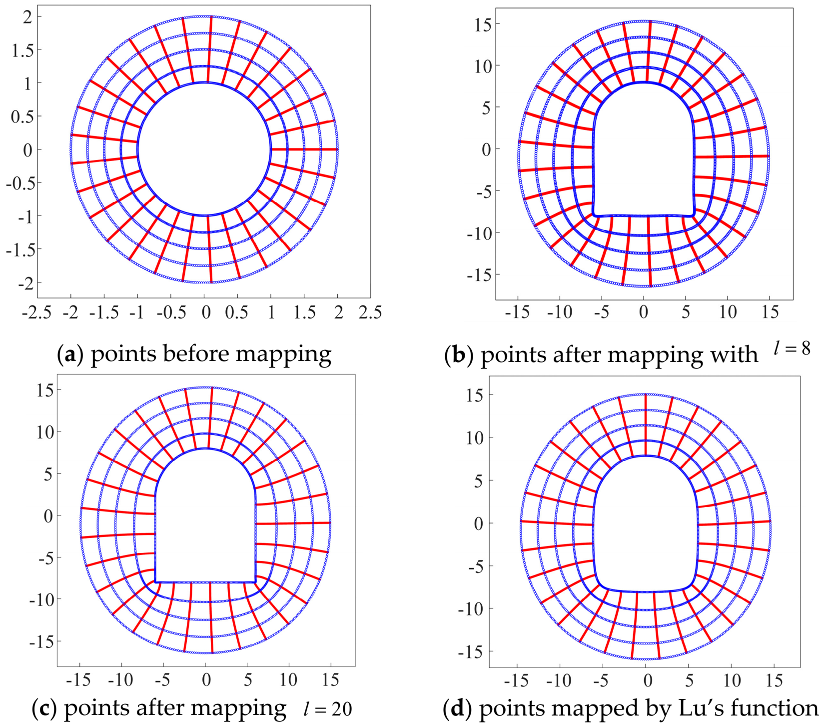


**Figure 40.** Illustration of approximate conformal mapping of the rock domain in Case 4.

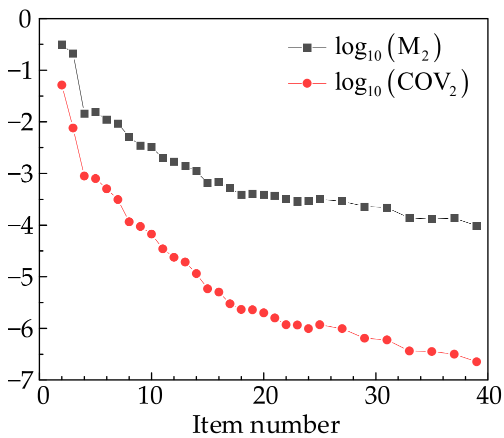


**Figure 41.** Approximation error for approximate conformal mapping of the rock domain in Case 3.

## 6. Conclusions

Initially, this paper reviews the literature on conformal mapping methods in the research of mechanical analysis in tunnel engineering. Three methods have been developed or adopted in these studies: optimization, iteration, and the extended Melentiev's methodology. These methods are erroneously thought to be effective in conformally mapping noncircular tunnel sections conformally. Through a detailed analysis and scrutiny, these methods turn out to be only the ordinary transformation function between the boundaries. More importantly, it is proven that these methods cannot guarantee the conformality of the mapping between rock cavity sections and circular domains according to the definition of conformal mapping, the existence and uniqueness theorem, and the boundary correspondence principle.

Consequently, the evolution of conformal mapping research in the complex analysis field is investigated thoroughly. The advanced SC formulas for multiply connected domains and related numerical methods are identified and chosen to develop the new procedure. By extending the discretization function for boundaries, the conformal mapping procedure for tunnels with polygonal boundaries, multi-arc boundaries, smooth curve boundaries, and mixed boundaries is proposed and programmed. Then, conformal mapping and inverse mapping of six typical tunnel cross sections buried at depth including rectangular holes, multiarc tunnels, horseshoe-shaped tunnels, and multiple holes are performed and illustrated in Case 1 to Case 6. The conformal mapping of the shallow cavities can be implemented using the symmetry principle of conformal mapping, as illustrated in Case 7.

Finally, tips on applying this procedure to the mechanical analysis study of irregularly shaped cavities are presented. The approximate conformal mappings of the rock domains in Case 3 and Case 4 are performed. The approximation error is significantly reduced by increasing the item number when approximating the conformal mapping based on a finite number of items of the power series. The contribution of this paper will be used not only in deriving analytical solutions of tunnels but also in the back analysis of tunnel mechanical behavior, which will be of great use for increasing the safety of tunnel engineering [121,122].

**Supplementary Materials:** Partial code is provided. The data that support the findings of this study are openly available in the main procedure of conformal mapping of lining in Case 4 at: https://drive.google.com/file/d/1fBJxl0kZoCIoO2wZZqCdiB6FLeVCuenD/view?usp=drive_link (accessed on 9 January 2024).

**Author Contributions:** Conceptualization, W.C., D.Z. and Q.F.; methodology, W.C.; software, W.C.; validation, W.C., D.Z., and Q.F.; formal analysis, W.C.; investigation, W.C. and X.C.; resources, W.C.; data curation, W.C. and D.Z.; writing—original draft preparation, W.C.; writing—review and editing, D.Z. and Q.F.; visualization, W.C., X.C. and L.Y.; supervision, D.Z. and Q.F.; project administration, W.C. and D.Z.; funding acquisition, W.C. and D.Z. All authors have read and agreed to the published version of the manuscript.

**Funding:** This project was funded by the Fundamental Research Funds for the Central Universities (Grant No. 2021YJS110), the National Key Research and Development Program of China (Grant No. 2017YFC0805401), and the National Natural Science Foundation of China (Grant No. 51738002).

**Data Availability Statement:** Data are contained within the article and Supplementary Materials.

**Acknowledgments:** The authors are grateful to both the funders and the editors' and reviewers' work, which improved the results and the presentation of this paper. Furthermore, the authors thank Darren A., Mohamed M. S. Nasser, and Thomas K. DeLillo et al. for their groundbreaking work in conformal mapping theory.

**Conflicts of Interest:** The authors declare no conflicts of interest.

## References

1. Muskhelishvili, N.I. *Some Basic Problems of the Mathematical Theory of Elasticity*; Springer: Dordrecht, The Netherlands, 1977. [CrossRef]
2. Strack, O.E. Analytic Solutions of Elastic Tunnelling Problems. Ph.D. Thesis, Delft University of Technology, Delft, The Netherlands, 2002; Available online: http://resolver.tudelft.nl/uuid:9f647e91-6496-4ba9-9b5d-63526c845789 (accessed on 1 July 2022).
3. Chen, Z.Y. *Analytical Method of Rock Mechanics Analysis*; China Coal Industry Publishing House: Beijing, China, 1994.
4. Lu, J.-K. *Complex Variable Methods in Plane Elasticity*; World Scientific: Singapore, 1995. [CrossRef]
5. Barber, J.R. *Elasticity*, 3rd ed.; Springer: Dordrecht, The Netherlands, 2010.
6. Kantorovich, L.V.; Krylov, V.I. *Approximate Methods of Higher Analysis*, 3rd ed.; Benster, C.D., Translator; Interscience Publisher: New York, NY, USA, 1958; Available online: http://books.google.com/books/about/Approximate_methods_of_higher_analysis.html?id=TKA8AAAAIAAJ&pgis=1 (accessed on 1 July 2022).
7. Melentiev, P. *Several New Methods and Devices for Approximate Computations*; Nordhoff: Groningen, The Netherlands, 1953.
8. Setiawan, N.B.; Zimmerman, R.W. A unified methodology for computing the stresses around an arbitrarily-shaped hole in isotropic or anisotropic materials. *Int. J. Solids Struct.* **2020**, *199*, 131–143. [CrossRef]
9. Setiawan, N.B.; Zimmerman, R.W. Semi-analytical Method for Modeling Wellbore Breakout Development. *Rock Mech. Rock Eng.* **2022**, *55*, 2987–3000. [CrossRef]
10. Zhang, D.; Xu, T.; Fang, H.; Fang, Q.; Cao, L.; Wen, M. Analytical modeling of complex contact behavior between rock mass and lining structure. *J. Rock Mech. Geotech. Eng.* **2021**, *14*, 813–824. [CrossRef]
11. Exadaktylos, G.; Liolios, P.; Stavropoulou, M. A semi-analytical elastic stress–displacement solution for notched circular openings in rocks. *Int. J. Solids Struct.* **2003**, *40*, 1165–1187. [CrossRef]

12. Huangfu, P.P.; Wu, F.Q.; Guo, S.F. A new method for calculating mapping function of external area of cavern with arbitrary shape based on searching points on boundary. *Rock Soil Mech.* **2011**, *32*, 1418–1424. [CrossRef]
13. Zhu, J.H.; Yang, J.H.; Shi, G.P.; Wang, J.; Cai, J.P. Calculating method for conformal mapping from exterior of unit circle to exterior of cavern with arbitrary excavation cross-section. *Rock Soil Mech.* **2014**, *35*, 175–183. [CrossRef]
14. Zhou, H.; Liu, H.; Yuan, J. A novel analytical approach for predicting the noncylindrical pile penetration-induced soil displacement in undrained soil by combining use of cavity expansion and strain path methods. *Int. J. Numer. Anal. Methods Geomech.* **2018**, *42*, 1270–1305. [CrossRef]
15. Xu, M.-F.; Wu, S.-C.; Gao, Y.-T.; Ma, J.; Wu, Q.-L. Analytical elastic stress solution and plastic zone estimation for a pressure-relief circular tunnel using complex variable methods. *Tunn. Undergr. Space Technol.* **2019**, *84*, 381–398. [CrossRef]
16. He, K.; Chang, J.; Pang, D.; Sun, B.; Yin, Z.; Li, D. Iterative algorithm for the conformal mapping function from the exterior of a roadway to the interior of a unit circle. *Arch. Appl. Mech.* **2022**, *92*, 971–991. [CrossRef]
17. Bu, W.; Xu, H.; Ji, M. An Analytical Elastic Solution for Right-Angle Trapezoidal Opening in Steeply Inclined Coal Seam. *Processes* **2022**, *10*, 110. [CrossRef]
18. Tan, L.; Ren, T.; Dou, L.; Yang, X.; Qiao, M.; Peng, H. Analytical stress solution and mechanical properties for rock mass containing a hole with complex shape. *Theor. Appl. Fract. Mech.* **2021**, *114*, 103002. [CrossRef]
19. Tan, L.; Wang, G.; Ren, T.; Dou, L.; Yang, X.; Song, S. Stress distribution and mechanical behaviour of rock mass containing two openings underground: Analytical and numerical studies. *Geofluids* **2021**, *2021*, 1917443. [CrossRef]
20. Tong, L.; Zhou, H.; Shen, H.; Liu, H. A Complex variable solution for shallow rectangular tunnel in semi-infinite plane. *J. Eng. Mech.* **2022**, *148*, 04022012. [CrossRef]
21. Lu, A.; Liu, Y.; Cai, H. A reasonable solution to the elastic problem of half-plane. *Meccanica* **2021**, *56*, 2169–2182. [CrossRef]
22. Zhang, Q.; Cheng, K.; Lin, C.; Lou, Y.; Guo, P.; Gan, X. Ground Displacements due to the deformations of shallow tunnels with arbitrary cross sections in soft ground. *Adv. Civ. Eng.* **2021**, *2021*, 9916159. [CrossRef]
23. Lu, A.Z. A New Method of Determintion of the Mapping Function for a Non-circle Tunnel with Full Support. *Chin. J. Geotech. Eng.* **1995**, *17*, 269–274.
24. Lu, A.Z.; Wang, Q.W. New method of determination for the mapping function of tunnel with arbitrary boundary using optimization techniques. *Chin. J. Rock Mech. Eng.* **1995**, *14*, 269–274.
25. Lu, A.Z.; Zhang, L.Q. *Complex Function Method on Mechanical Analysis of Underground Tunnel*; Science Press: Beijing, China, 2007; Available online: https://book.sciencereading.cn/shop/book/Booksimple/show.do?id=BDEB0784367A948FDB66734E9D8B4CE90000 (accessed on 8 August 2022).
26. Luqing, Z.; Zhifa, Y.; Aizhong, L. Analytics study on the problem of two holes having arbitrary shapes and arrangements in plane elastostatics. *Sci. China Ser. D Earth Sci.* **2001**, *44*, 146–158. [CrossRef]
27. Qi, C.; Fourie, A.; Chen, Q.; Dong, X. Analytical solution for stress distribution around arbitrary stopes using evolutionary complex variable methods. *Int. J. Geomech.* **2019**, *19*, 04019113. [CrossRef]
28. Li, X.Y.; Liu, G.B. Calculating method for conformal mapping from exterior of cavern with arbitrary excavation cross-section in half-plane to the area between two concentric circles. *Chin. J. Rock Mech. Eng.* **2018**, *37*, 3507–3514. [CrossRef]
29. Wu, H.; Zhao, G.; Liang, W. Investigation of cracking behavior and mechanism of sandstone specimens with a hole under compression. *Int. J. Mech. Sci.* **2019**, *163*, 105084. [CrossRef]
30. Wu, H.; Zhao, G.; Liang, W. Mechanical properties and fracture characteristics of pre-holed rocks subjected to uniaxial loading: A comparative analysis of five hole shapes. *Theor. Appl. Fract. Mech.* **2019**, *105*, 102433. [CrossRef]
31. Tan, L.; Ren, T.; Dou, L.; Yang, X.; Wang, G.; Peng, H. Analytical stress solution and numerical mechanical behavior of rock Mass containing an opening under different confining stress conditions. *Mathematics* **2021**, *9*, 2462. [CrossRef]
32. Ye, Z.K.; Ai, Z.Y. A novel complex variable solution for the stress and displacement fields around a shallow non-circular tunnel. *Comput. Geotech.* **2023**, *164*, 105797. [CrossRef]
33. Lu, A.-Z.; Zhang, N.; Kuang, L. Analytic solutions of stress and displacement for a non-circular tunnel at great depth including support delay. *Int. J. Rock Mech. Min. Sci.* **2014**, *70*, 69–81. [CrossRef]
34. Lu, A.-Z.; Zhang, N.; Qin, Y. Analytical solutions for the stress of a lined non-circular tunnel under full-slip contact conditions. *Int. J. Rock Mech. Min. Sci.* **2015**, *79*, 183–192. [CrossRef]
35. Han, X.; Xia, Y. Analytic Solutions of the Forces and Displacements for Multicentre Circular Arc Tunnels. *Math. Probl. Eng.* **2018**, *2018*, 8409129. [CrossRef]
36. Li, Y.; Chen, S. A complex variable solution for lining stress and deformation in a non-circular deep tunnel II practical application and verification. *Math. Comput. Appl.* **2018**, *23*, 43. [CrossRef]
37. Lu, A.; Wang, S.; Zhang, X.; Zhang, N. Solution of the elasto-plastic interface of circular tunnels in Hoek–Brown media subjected to non-hydrostatic stress. *Int. J. Rock Mech. Min. Sci.* **2018**, *106*, 124–132. [CrossRef]
38. Ma, Y.; Lu, A.; Cai, H. An analytical method for determining the non-enclosed elastoplastic interface of a circular hole. *Math. Mech. Solids* **2020**, *25*, 1199–1213. [CrossRef]
39. Li, Y.S.; Chen, S.G. Analytical solution of frost heaving force in non-circular cold region tunnels. *Chin. J. Theor. Appl. Mech.* **2020**, *52*, 196–207. [CrossRef]
40. Li, Y.S.; Chen, S.G. Analytical solution of stress and deformation of noncircular tunnel considering grouting circle. *Zhongguo Gonglu Xuebao/China J. Highw. Transp.* **2018**, *31*, 255.

41. Zhu, Y.; Li, Y.; Hao, Z.; Luo, L.; Luo, J.; Wang, L. An analytical solution for the frost heaving force and displacement of a noncircular tunnel. *Comput. Geotech.* **2021**, *133*, 104022. [CrossRef]
42. Zeng, X.T.; Lu, A.Z. Analytical stress solution research on an infinte plate contianing two non-circular holes. *Lixue Xuebao/Chin. J. Theor. Appl. Mech.* **2019**, *51*, 170–181. [CrossRef]
43. Wang, H.N.; Jiang, M.J.; Zhao, T.; Zeng, G.S. Viscoelastic solutions for stresses and displacements around non-circular tunnels sequentially excavated at great depths. *Acta Geotech.* **2019**, *14*, 111–139. [CrossRef]
44. Zeng, G.; Wang, H.; Jiang, M. Analytical solutions of noncircular tunnels in viscoelastic semi-infinite ground subjected to surcharge loadings. *Appl. Math. Model.* **2022**, *102*, 492–510. [CrossRef]
45. Zhao, Y.; Zhang, J.; Li, L.; Hu, T.; Zhao, Y. Analytical solution for the temperature field of an elliptical tunnel in cold regions. *Cold Reg. Sci. Technol.* **2023**, *208*, 103793. [CrossRef]
46. Zeng, G.-S.; Cai, H.; Lu, A.-Z. An Analytical Solution for an Arbitrary Cavity in an Elastic Half-Plane. *Rock Mech. Rock Eng.* **2019**, *52*, 4509–4526. [CrossRef]
47. Fang, H.; Zhang, D.; Fang, Q. A semi-analytical method for frictional contact analysis between rock mass and concrete linings. *Appl. Math. Model.* **2022**, *105*, 17–28. [CrossRef]
48. Fang, H.; Zhang, D.; Fang, Q.; Wen, M. A generalized complex variable method for multiple tunnels at great depth considering the interaction between linings and surrounding rock. *Comput. Geotech.* **2021**, *129*, 103891. [CrossRef]
49. Fang, H.C.; Zhang, D.L.; Wen, M. A non-iterative analytical method for mechanical analysis of surrounding rock with arbitrary shape holes. *Chin. J. Rock Mech. Eng.* **2020**, *39*, 2204–2212. [CrossRef]
50. Kargar, A.R.; Haghgouei, H. An analytical solution for time-dependent stress field of lined circular tunnels using complex potential functions in a stepwise procedure. *Appl. Math. Model.* **2020**, *77*, 1625–1642. [CrossRef]
51. Kargar, A.; Rahmannejad, R.; Hajabasi, M. A semi-analytical elastic solution for stress field of lined non-circular tunnels at great depth using complex variable method. *Int. J. Solids Struct.* **2014**, *51*, 1475–1482. [CrossRef]
52. Li, Y.S.; Chen, S.G. Lining and surrounding rock in non-circular tunnel based on complex variable method. *Xinan Jiaotong Daxue Xuebao/J. Southwest Jiaotong Univ.* **2020**, *55*, 265–272. [CrossRef]
53. Yu, Y.; Tang, L.; Ling, X.; Geng, L.; Wei, S.; Zhou, G. Investigation of the soil-lining interaction at a tunnel entrance during freeze-thaw cycling: Model testing and semi-empirical modeling. *Tunn. Undergr. Space Technol.* **2021**, *115*, 104028. [CrossRef]
54. Orloff, J. Complex Variables with Applications: Chapter 11, (2021) 11.1.1-11.1.1. Available online: https://math.libretexts.org/Bookshelves/Analysis/Complex_Variables_with_Applications_(Orloff)/11:_Conformal_Transformations/11.01:_Geometric_Definition_of_Conformal_Mappings (accessed on 8 August 2022).
55. Andrei, B.; Ludmila, B. *Complex Analysis*; Springer: Singapore, 2021. [CrossRef]
56. Wen, G.C. *Conformal Mappings and Boundary Value Problems*; English Translation of Chinese Edition 1984; American Mathematical Society: Providence, RI, USA, 1992.
57. Ivanov, V.I.; Trubetskov, M.K. *Handbook of Conformal Mapping with Computer-Aided Visualization*; CRC Press: Boca Raton, FL, USA, 1995.
58. Zhang, X.; Lu, A.; Song, K.; Wu, G.; Wang, L. Methodology for Determining the Compliance Matrix and Analyzing the Skew Anisotropic Plate with an Arbitrarily Shaped Hole. *Adv. Mater. Sci. Eng.* **2022**, *2022*, 5949398. [CrossRef]
59. Cui, J.B.; Ji, A.Z.; Xiong, G.M. Research on surrounding rock stress distributions for circular tunnels based on the Schwarz-Christoffel Transformation. *Appl. Math. Mech.* **2019**, *40*, 1089–1098. [CrossRef]
60. Xiong, X.; Dai, J.; Xinnian, C.; Ouyang, Y. Complex function solution for deformation and failure mechanism of inclined coal seam roadway. *Sci. Rep.* **2022**, *12*, 7147. [CrossRef]
61. Crowdy, D. The Schwarz–Christoffel mapping to bounded multiply connected polygonal domains. *Proc. R. Soc. A Math. Phys. Eng. Sci.* **2005**, *461*, 2653–2678. [CrossRef]
62. Crowdy, D. Schwarz–Christoffel mappings to unbounded multiply connected polygonal regions. *Math. Proc. Camb. Philos. Soc.* **2007**, *142*, 319–339. [CrossRef]
63. DeLillo, T.K.; Elcrat, A.R.; Pfaltzgraff, J.A. Schwarz–Christoffel Mapping of the Annulus. *SIAM Rev.* **2001**, *43*, 469–477. [CrossRef]
64. Kargar, A.R.; Rahmannejad, R.; Hajabasi, M.A. The stress state around lined non-circular hydraulic tunnels below the water table using complex variable method. *Int. J. Rock Mech. Min. Sci.* **2015**, *78*, 207–216. [CrossRef]
65. Lavrik, V.I.; Savenkov, V.N. *A Handbook on Conformal Mappings*; Naukova Dumka: Kiev, Ukraine, 1970.
66. Nehari, Z. *Conformal Mapping*; Dover Publications, INC.: New York, NY, USA, 1975.
67. Wegmann, R. Ein Iterationsverfahren zur konformen Abbildung. *Numer. Math.* **1978**, *30*, 453–466. [CrossRef]
68. Wegmann, R. An iterative method for conformal mapping. *J. Comput. Appl. Math.* **1986**, *14*, 7–18. [CrossRef]
69. Henrici, P. *Applied and Computational Complex Analysis*; Wiley: New York, NY, USA, 1986.
70. Schinzinger, R.; Laura, P.A.A. *Conformal Mapping: Methods and Applications*; Elsevier: Amsterdam, The Netherlands, 1991.
71. Kythe, P.K. *Computational Conformal Mapping*; Birkhäuser: Boston, MA, USA, 1998.
72. Driscoll, T.A.; Trefethen, L.N. *Schwarz-Christoffel Mapping*; Cambridge University Press: Cambridge, UK, 2002.
73. Wegmann, R. Methods for numerical conformal mapping: Dedicated to the memory of Dieter Gaier. In *Handbook of Complex Analysis: Geometric Function Theory*; Elsevier: Amsterdam, The Netherlands, 2005; Volume 2, pp. 351–477. [CrossRef]
74. Delillo, T.K.; Elcrat, A.R.; Pfaltzgraff, J.A. Schwarz-Christoffel mapping of multiply connected domains. *J. Anal. Math.* **2004**, *94*, 17–47. [CrossRef]

75. DeLillo, T.K. Schwarz-Christoffel Mapping of Bounded, Multiply Connected Domains. *Comput. Methods Funct. Theory* **2006**, *6*, 275–300. [CrossRef]
76. Crowdy, D. The Schottky-Klein Prime Function on the Schottky Double of Planar Domains. *Comput. Methods Funct. Theory* **2010**, *10*, 501–517. [CrossRef]
77. Crowdy, D. *Solving Problems in Multiply Connected Domains, NSF-CBMS Regional Conference Series in Applied Mathematics*; SIAM: Philadelphia, PA, USA, 2020. [CrossRef]
78. Bauer, U.J. *Conformal Mappings Onto Simply and Multiply Connected Circular Arc Polygon Domains*; Universität Würzburg: Würzburg, German, 2015.
79. Kythe, P.K. *Handbook of Conformal Mappings and Applications*; CRC Press: Boca Raton, FL, USA, 2019.
80. Wegmann, R. Constructive solution of a certain class of Riemann–Hilbert problems on multiply connected circular regions. *J. Comput. Appl. Math.* **2001**, *130*, 139–161. [CrossRef]
81. Wegmann, R.; Murid, A.; Nasser, M. The Riemann–Hilbert problem and the generalized Neumann kernel. *J. Comput. Appl. Math.* **2005**, *182*, 388–415. [CrossRef]
82. Wegmann, R.; Nasser, M.M. The Riemann–Hilbert problem and the generalized Neumann kernel on multiply connected regions. *J. Comput. Appl. Math.* **2008**, *214*, 36–57. [CrossRef]
83. Nasser, M.M.S. A nonlinear integral equation for numerical conformal mapping. *Adv. Pure Appl. Math.* **2010**, *1*, 47–63. [CrossRef]
84. Nasser, M.M.S. Fast solution of boundary integral equations with the generalized Neumann kernel. *arXiv* **2013**, arXiv:1308.5351. [CrossRef]
85. Nasser, M.M.S. Fast Computation of the Circular Map. *Comput. Methods Funct. Theory* **2015**, *15*, 187–223. [CrossRef]
86. Nasser, M.M.S.; Murid, A.H.M.; Sangawi, A.W.K. Numerical conformal mapping via a boundary integral equation with the adjoint generalized Neumann kernel. *arXiv* **2013**, arXiv:1308.3929. [CrossRef]
87. Nasser, M.M.S.; Al-Shihri, F.A.A. A Fast Boundary Integral Equation Method for Conformal Mapping of Multiply Connected Regions. *SIAM J. Sci. Comput.* **2013**, *35*, A1736–A1760. [CrossRef]
88. Al-Hatemi, S.A.; Murid, A.H.; Nasser, M.M. Solving a mixed boundary value problem via an integral equation with adjoint generalized Neumann kernel in bounded multiply connected regions. In *AIP Conference Proceedings*; American Institute of Physics: Johor Bahru, Malaysia, 2013; pp. 508–517. [CrossRef]
89. Nasser, M.M. Numerical conformal mapping of multiply connected regions onto the fifth category of Koebe's canonical slit regions. *J. Math. Anal. Appl.* **2013**, *398*, 729–743. [CrossRef]
90. DeLillo, T.K.; Kropf, E.H. Numerical Computation of the Schwarz–Christoffel Transformation for Multiply Connected Domains. *SIAM J. Sci. Comput.* **2011**, *33*, 1369–1394. [CrossRef]
91. Yunus, A.A.M.; Murid, A.H.M.; Nasser, M.M.S. Numerical evaluation of conformal mapping and its inverse for unbounded multiply connected regions. *Bull. Malays. Math. Sci. Soc.* **2014**, *37*, 1–24.
92. Luo, W.; Dai, J.; Gu, X.; Yau, S.-T. Numerical conformal mapping of multiply connected domains to regions with circular boundaries. *J. Comput. Appl. Math.* **2010**, *233*, 2940–2947. [CrossRef]
93. Liesen, J.; Sète, O.; Nasser, M.M.S. Fast and Accurate Computation of the Logarithmic Capacity of Compact Sets. *Comput. Methods Funct. Theory* **2017**, *17*, 689–713. [CrossRef]
94. Gopal, A.; Trefethen, L.N. Representation of conformal maps by rational functions. *Numer. Math.* **2019**, *142*, 359–382. [CrossRef]
95. Trefethen, L.N. Numerical Conformal Mapping with Rational Functions. *Comput. Methods Funct. Theory* **2020**, *20*, 369–387. [CrossRef]
96. Trefethen, L.N. *SCPACK User's Guide*; Numerical Analysis Report 89-2; MIT Department of Mathematics: Cambridge, MA, USA, 1989.
97. Trefethen, L.N. Numerical Computation of the Schwarz–Christoffel Transformation. *SIAM J. Sci. Stat. Comput.* **1980**, *1*, 82–102. [CrossRef]
98. Driscoll, T.A. Algorithm 756: A MATLAB toolbox for Schwarz-Christoffel mapping. *ACM Trans. Math. Softw.* **1996**, *22*, 168–186. [CrossRef]
99. Driscoll, T.A. Algorithm 843: Improvements to the Schwarz-Christoffel toolbox for MATLAB. *ACM Trans. Math. Softw.* **2005**, *31*, 239–251. [CrossRef]
100. Driscoll, T.A. Schwarz–Christoffel Toolbox. 2019. Available online: https://github.com/tobydriscoll/sc-toolbox (accessed on 8 August 2022).
101. Nasser, M.M. PlgCirMap: A MATLAB toolbox for computing conformal mappings from polygonal multiply connected domains onto circular domains. *SoftwareX* **2020**, *11*, 100464. [CrossRef]
102. Nasser, M.M. Numerical conformal mapping of multiply connected regions onto the second, third and fourth categories of Koebe's canonical slit domains. *J. Math. Anal. Appl.* **2011**, *382*, 47–56. [CrossRef]
103. Nasser, M.; Murid, A.; Ismail, M.; Alejaily, E. Boundary integral equations with the generalized Neumann kernel for Laplace's equation in multiply connected regions. *Appl. Math. Comput.* **2011**, *217*, 4710–4727. [CrossRef]
104. Mayo, A. Rapid methods for the conformal mapping of multiply connected regions. *J. Comput. Appl. Math.* **1986**, *14*, 143–153. [CrossRef]
105. Kress, R. A Nyström method for boundary integral equations in domains with corners. *Numer. Math.* **1990**, *58*, 145–161. [CrossRef]

106. Jeon, Y. A Nyström Method for Boundary Integral Equations on Domains with a Piecewise Smooth Boundary. *J. Integral Equations Appl.* **1993**, *5*, 221–242. [CrossRef]
107. Verruijt, A. A complex variable solution for a deforming circular tunnel in an elastic half-plane. *Int. J. Numer. Anal. Methods Geomech.* **1997**, *21*, 77–89. [CrossRef]
108. Lin, L.-B.; Lu, Y.-P.; Chen, F.-Q.; Li, D.-Y. Analytic study of stress and displacement for shallow twin tunnels subjected to surcharge loads. *Appl. Math. Model.* **2021**, *93*, 485–508. [CrossRef]
109. Guo, Y.; Wang, H.; Jiang, M. Efficient Iterative Analytical Model for Underground Seepage around Multiple Tunnels in Semi-Infinite Saturated Media. *J. Eng. Mech.* **2021**, *147*, 04021101. [CrossRef]
110. Lin, L.-B.; Chen, F.-Q.; Lu, Y.-P.; Li, D.-Y. Complex variable solutions for shallow twin tunnelling in visco-elastic geomaterial considering buoyancy effect and equivalent three-dimensional effects of tunnel faces. *Appl. Math. Model.* **2021**, *91*, 149–185. [CrossRef]
111. Samal, K.P.; Mishra, G.C. Analysis of seepage from a triangular furrow considering soil capillarity using inverse hodograph and conformal mapping technique. *ISH J. Hydraul. Eng.* **2017**, *23*, 1–12. [CrossRef]
112. Wang, L.-Z.; Li, L.-L.; Lv, X.-J. Complex Variable Solutions for Tunneling-Induced Ground Movement. *Int. J. Geomech.* **2009**, *9*, 63–72. [CrossRef]
113. Zeng, G.; Wang, H.; Jiang, M. Analytical study of ground responses induced by the excavation of quasirectangular tunnels at shallow depths. *Int. J. Numer. Anal. Methods Geomech.* **2019**, *43*, 2200–2223. [CrossRef]
114. Zeng, G.S.; Wang, H.N.; Wu, L.; Jiang, M.J. A Generalized Analytical Model for Mechanical Responses of Rock during Multiple-Tunnel Excavation in Viscoelastic Semi-Infinite Ground. *Int. J. Geomech.* **2021**, *21*, 04021202. [CrossRef]
115. Chen, W.B.; Fang, Q.; Zhang, D.L.; Chen, X.H. Mechanical analysis method for deep buried non-circular tunnel considering conformal mapping difference between rock and lining. *J. Cent. South Univ. Sci. Technol.* **2023**, *6*, 2349–2359. [CrossRef]
116. Zhang, Z.; Sun, Y. Analytical solution for a deep tunnel with arbitrary cross section in a transversely isotropic rock mass. *Int. J. Rock Mech. Min. Sci.* **2011**, *48*, 1359–1363. [CrossRef]
117. Wang, H.; Zeng, G.; Jiang, M. Analytical stress and displacement around non-circular tunnels in semi-infinite ground. *Appl. Math. Model.* **2018**, *63*, 303–328. [CrossRef]
118. Lu, D.; Kong, F.; Du, X.; Shen, C.; Gong, Q.; Li, P. A unified displacement function to analytically predict ground deformation of shallow tunnel. *Tunn. Undergr. Space Technol.* **2019**, *88*, 129–143. [CrossRef]
119. Hua, J.; Dai, M. Anti-plane shear of a tunnel in an elastic half-space under surface loading: Analytic algorithm and approximate explicit solution. *Discret. Contin. Dyn. Syst.* **2022**, *73*, 42. [CrossRef]
120. Deng, T.; Wu, L.; Lin, J. Complex Variable Solution for a Tunnel Excavation Problem by Considering Lining Inner Pressure. In *Tunneling and Underground Construction*; American Society of Civil Engineers: Reston, VA, USA, 2014; pp. 116–124. [CrossRef]
121. Domaneschi, M.; Casciati, S.; Catbas, N.; Cimellaro, G.P.; Inaudi, D.; Marano, G.C. Structural health monitoring of in-service tunnels. *Int. J. Sustain. Mater. Struct. Syst.* **2020**, *4*, 268. [CrossRef]
122. Rosso, M.M.; Aloisio, A.; Randazzo, V.; Tanzi, L.; Cirrincione, G.; Marano, G.C. Comparative deep learning studies for indirect tunnel monitoring with and without Fourier pre-processing. *Integr. Comput. Eng.* **2023**, 1–20. [CrossRef]